



Understanding 3D genome organization by multidisciplinary methods

Ivana Jerković and Giacomo Cavalli

Abstract | Understanding how chromatin is folded in the nucleus is fundamental to understanding its function. Although 3D genome organization has been historically difficult to study owing to a lack of relevant methodologies, major technological breakthroughs in genome-wide mapping of chromatin contacts and advances in imaging technologies in the twenty-first century considerably improved our understanding of chromosome conformation and nuclear architecture. In this Review, we discuss methods of 3D genome organization analysis, including sequencing-based techniques, such as Hi-C and its derivatives, Micro-C, DamID and others; microscopy-based techniques, such as super-resolution imaging coupled with fluorescence in situ hybridization (FISH), multiplex FISH, in situ genome sequencing and live microscopy methods; and computational and modelling approaches. We describe the most commonly used techniques and their contribution to our current knowledge of nuclear architecture and, finally, we provide a perspective on up-and-coming methods that open possibilities for future major discoveries.

Euchromatin, heterochromatin and the hypothesis of individual-chromosome territories in the nucleus were already observed and suggested at the end of the nineteenth and the beginning of the twentieth century using light microscopy and chromatin dyes^{1–3}. However, by the middle of the twentieth century, the chromosome territories hypothesis was largely abandoned as conventional electron microscopy failed to confirm it. It was not until the 1980s and the development of a novel imaging technique named fluorescence in situ hybridization (FISH) that the chromosome territories hypothesis was finally validated, thereby instigating the study of nuclear architecture as we know it today^{4–6}. The FISH method demonstrated the existence of chromosome territories and chromosome intermingling at territory edges, and also indicated that chromosomal regions rich in active genes largely reside in the nuclear interior, whereas chromosomal regions rich in inactive genes largely reside in the nuclear periphery^{7–16}.

About two decades later, completion of sequencing of the human genome and the subsequent genome-wide characterization of genetic variations and epigenetic transcription regulation propelled the study of nuclear architecture into a new era. One breakthrough was the development of new techniques based on the principles of ligation of linearly distal genomic regions that come into 3D spatial proximity in order to map genome organization and, at the same time, assay the functionality of this 3D organization^{17,18}. However, despite the

tremendous advancements made in this relatively short time, the full complexity of the biophysical principles underlying the strong 3D compaction of the long linear genomic DNA into a micrometre-sized nucleus remains to be elucidated. Furthermore, we do not know the rules by which the structures imposed by general biophysical laws can be modified at specific genes in order to drive changes in gene expression programmes that underlie cell fate and plasticity. These major challenges stimulate methodological improvements and invention of new experimental techniques and modelling approaches. On the other hand, fast and numerous technical developments generate confusion in the field of genome organization research, as it is unclear what information can each method provide, and the scarce comparison of concurrent methods hampers progress. Given the technological challenges and limitations of each of technology, the multiscale nature of genome organization and the multifaceted regulation of genome function, only deployment of the full discourse of experimental and theoretical genome analysis approaches will allow us to reach a complete appreciation of genome function and the capacity to harness it in order to deliver not only fundamental knowledge but also valuable biomedical applications.

In this Review, we discuss techniques for high-throughput chromatin contacts analysis and highly multiplexed, super-resolution and live-imaging methods. The applicability of these techniques is intimately linked

Institute of Human Genetics, CNRS, University of Montpellier, Montpellier, France.

e-mail: giacomo.cavalli@igh.cnrs.fr

<https://doi.org/10.1038/s41580-021-00362-w>

First principles

Basic building blocks of knowledge that cannot be deduced from any other preposition used for mathematical modelling of polymer behaviours.

Loop-extrusion model

A model suggesting that motor protein complexes such as cohesin or condensin form around chromatin and use the energy of ATP to slide through it while extruding the intervening region.

Tyramide signal amplification

(TSA). A method enabling sensitive detection of low-abundance molecules in fluorescent immunocytochemistry applications.

Multiway contacts

Chromatin contacts involving more than two chromatin fragments.

Nuclear speckles

Nuclear foci enriched in pre-mRNA splicing factors.

with computational tools, including machine learning and mathematical modelling based on first principles or driven by quantitative data. We discuss relevant technological progress, provide a view of the current state of 3D genome organization research and discuss promising future developments.

Studying the multilayered 3D genome

The idea of the nucleus as a highly organized organelle existed for over a century^{1–3}. However, so far, we grasp only a part of the principles that govern nuclear organization, and the emergence of new evidence is tightly connected with the development of new methods.

A major breakthrough in chromatin biology was the establishment of chromosome conformation capture (3C) — a nuclear ligation assay in conjunction with PCR that marked the beginning of the era of high-throughput next-generation sequencing-based techniques for the investigation of chromosome conformation^{17,18}. Indeed, a series of 3C derivatives (from here on defined as C-based techniques) were developed to assay contact frequency between multiple genomic loci, including circular 3C (4C)¹⁹, which measures interaction frequencies of one locus with many loci ('one versus many'), many versus many assays (3C carbon copy (5C)²⁰, Capture-C^{21–25}, Capture-Hi-C²⁶ and so on) and genome-wide, all versus all assays^{27,28} such as Hi-C²⁹ (BOX 1). Progressively, these techniques were tweaked to allow for enrichment of specific contacts driven by proteins of interest (many versus all), including chromatin immunoprecipitation (ChIP-loop)³⁰, chromatin interaction analysis with paired-end tag (ChIA-PET)³¹, HiChIP³² and proximity ligation-assisted ChIP followed by sequencing

(PLAC-seq)³³, or for enrichment of contacts focused on selected genomic locations (Capture-C^{21–25} and Capture-Hi-C²⁶)²⁹.

Simultaneously with the development of the C-based techniques, ligation-independent techniques were invented to assay not only chromosome conformation in general but also the nuclear position of chromatin contacts (tyramide signal amplification (TSA), DNA adenine methyltransferase identification (DamID) and split-pool recognition of interactions by tag extension (SPRITE)) and multiway contacts (SPRITE and genome architecture mapping (GAM)), which are not assayed effectively using ligation-based techniques^{34–42}. Finally, the recent advancement of super-resolution microscopy and imaging techniques allowed us to investigate chromatin conformation of single cells at extremely high resolution and at a higher throughput than ever before^{12,14,15,43–48}. In addition to improvements in spatial resolution, live imaging in combination with genome engineering using CRISPR-Cas9 systems facilitated and improved the study of chromatin contact dynamics^{49–51}.

Owing to these methodological and technological advancements, it is not surprising that the past decade has provided major revelations in 3D genome organization and function. Most notable is the finding that chromosomes in interphase predominantly fold into two compartments, A and B, which respectively consist of predominantly gene-active and gene-inactive regions²⁷ (FIG. 1). Furthermore, parts of compartments, from the same or different chromosomes, can come together and create hubs, which are connected by multiple chromatin interactions, thereby sharing a common function (for example, gene repression) and coalescing around different nuclear bodies such as nuclear speckles^{35,37,52}. On a scale below the compartments, chromatin interactions were found to be enriched within domains 100 kb–1 Mb in length termed topologically associating domains (TADs); these partially insulated domains are subdivided into smaller chromatin nanodomains (CNDs)^{43,53–57} (FIG. 1). Both of these layers of organization — compartments and TADs/CNDs — were confirmed to be genomic features present across cell lines and species, but the principles that govern their folding are just beginning to be elucidated^{58–66}. Chromatin loop extrusion is one mechanism responsible for folding at the megabase scale. In interphase, loop extrusion is mediated by cohesin complexes, which can be blocked by CCCTC-binding factor (CTCF) bound to sequence motifs in convergent orientation, thereby demarcating TAD boundaries^{58,59,61,62,64,67–75} (FIG. 1). Importantly, these features are not only structural in nature but are functional as well, as compartments quite homogeneously comprise gene-active or gene-inactive regions and TADs can facilitate the formation of enhancer-promoter contacts within their borders (BOX 2; FIG. 1). Although it is not entirely clear what the relationship is between TAD boundaries, insulation and disease, structural variations perturbing TAD boundaries and changes in CTCF binding and insulation can alter gene expression and lead to developmental defects and disease^{76–84} (BOX 2). These exemplary findings clearly demonstrate the importance of method development and choice in studying 3D

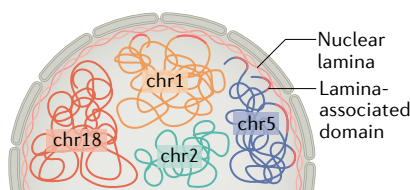
Box 1 | Proximity ligation-based methods for mapping chromatin interactions

The development of chromosome conformation capture (3C), which detects pairwise interactions between select loci ('one versus one') through nuclear-proximity ligation in combination with semi-quantitative PCR, marks the onset of the eponymous C-based techniques in the early 2000s^{17,18,29}. Using 3C, the locus control region of the β -globin locus was shown for the first time to form chromatin loops with, and thus to activate, its promoter and to form an active chromatin hub that dynamically follows transcription during differentiation and is stabilized by transcription factors^{220–223}. However, 3C is of low throughput and cannot successfully detect long-distance contacts. Circular 3C (4C) overcame these limitations by using primers in order to detect genome-wide contacts formed with a single 'viewpoint' (one versus all)^{19,224,225}. Later, 4C was combined with next-generation sequencing and was used to describe the dynamics of chromatin contacts during development^{226–229}. However, the most influential technique in 3D genome organization research is Hi-C, in which the DNA interactome of the entire genome is assayed (all versus all)²⁷. Hi-C led to the identification of genomic compartments and topologically associating domains and to the development of the loop-extrusion model^{27,53–55,58,59,61,64,67,85,130}. Finally, several techniques were developed, which combined Hi-C with chromatin immunoprecipitation, thereby allowing the interrogation of chromatin contact frequencies based on the presence of a specific protein^{31–33}. It is important to note that in all C-based techniques that include protein enrichment, the mapped contacts are probabilistic rather than deterministic features and it is impossible to predict how and whether these contacts will translate into function.

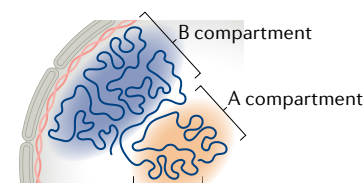
Together, proximity-ligation based techniques fuelled most of the discoveries in 3D genome organization research during the past 15 years. The ease of application of these techniques is anti-correlated with the richness of data obtained from them, which is likely the reason why so many different C-based technique adaptations exist. With the recent development of microscopy-related techniques, the proximity ligation-based data are even more valuable as they will offer imaging-complementary information that is invaluable for achieving a better understanding of genome folding.

Size **Organization level**

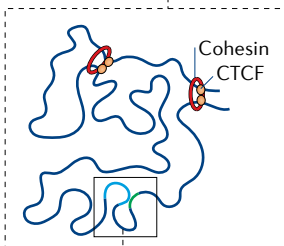
Entire chromosomes Chromosome territories



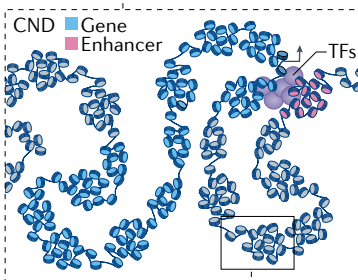
Up to 100s of megabases • Compartments
 • Hubs



100 kb to few megabases • Topologically associating domains
 • Chromatin loops



10–100 kb • Chromatin nanodomains
 • Functional loops (E–P contacts)



~1–2 kb Nucleosome clutches

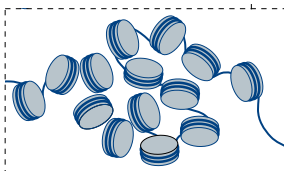


Fig. 1 | Multiple levels of genome organization and the methods to study them. DNA folds at multiple scales (indicated on the left) to build chromosomes. DNA winding around histones forms nucleosomes, which are organized into clutches, each containing ~1–2 kb of DNA¹¹⁶. Nucleosome clutches form chromatin nanodomains (CNDs) ~100 kb in size, where most enhancer–promoter (E–P) contacts take place^{43,57,117}. At the scale of ~1 Mb, CNDs and CCCTC-binding factor (CTCF)–cohesin-dependent chromatin loops form topologically associating domains (TADs)^{43,57,58,67,116,213,214}. On the higher scale up to 100s of megabases, chromatin segregates into gene-active and gene-inactive compartments (A and B, respectively) and into compartment-specific contact hubs (not shown). At the highest topological level, the nucleus is organized into chromosome territories^{27,35}. Different techniques can be used to study different genome organization levels, and some techniques can be used to study several organization levels. Although Hi-C, genome architecture mapping (GAM) and other sequencing-based techniques can be used to detect chromosome territories, 3D fluorescence in situ hybridization (FISH) is most useful to study this level of organization, as it provides direct spatial information^{7,27,41}. Compartments and hubs are usually studied with Hi-C, GAM, split-pool recognition of interactions by tag

extension (SPRITE) and several multiplexed super-resolution FISH techniques^{14,15,27,35,41,44–48,123}. At the more functional 1-Mb scale, most informative are capture Hi-C (cHi-C), Capture-C, micrococcal nuclease chromosome conformation assay (Micro-C) and super-resolution FISH approaches^{21–26,91}. Protein-driven enrichment techniques such as Hi-C chromatin immunoprecipitation (HiChIP), chromatin interaction analysis by paired-end tag sequencing (ChIA-PET), proximity ligation-assisted chromatin immunoprecipitation (ChIP) followed by sequencing (PLAC-seq) and chromatin-interaction analysis via droplet-based and barcode-linked sequencing (ChIA-Drop) can be used to study different levels of folding depending on whether the protein is associated with relatively local folding (for example, MED12 in E–P contacts), more long-range contacts (for example, Polycomb proteins) or inter-chromosomal hubs (for example, LHX2, LDB1)^{31–33,102,192,215–218}. CNDs have been discovered only recently. Owing to their stochastic nature and inter-cell variability, only super-resolution microscopy FISH has so far been able to detect CNDs^{43,57,117}. 4C, circular chromosome conformation capture; DamID, DNA adenine methyltransferase identification; GPSeq, genomic loci positioning by sequencing; TFs, transcription factors; TSA, tyramide signal amplification.

Methods		
Sequencing-based		Microscopy
Enrichment	Non-enrichment	
	<ul style="list-style-type: none"> • GAM • GPSeq 	3D FISH
<ul style="list-style-type: none"> • DamID • TSA-seq • ChIA-PET • ChIA-Drop 	<ul style="list-style-type: none"> • GAM • Hi-C • Micro-C • GPSeq • SPRITE 	<ul style="list-style-type: none"> • Super-resolution FISH • Electron microscopy
<ul style="list-style-type: none"> • Capture-C • cHi-C • 4C • ChIA-PET • ChIA-Drop • HiChIP • PLAC-seq 	<ul style="list-style-type: none"> • GAM • SPRITE • Hi-C • Micro-C 	Super-resolution FISH
<ul style="list-style-type: none"> • Capture-C • cHi-C • 4C • ChIA-PET • ChIA-Drop • HiChIP • PLAC-seq 	<ul style="list-style-type: none"> • GAM • Micro-C 	Super-resolution FISH
	Micro-C	<ul style="list-style-type: none"> • Super-resolution FISH • Electron microscopy

Polycomb

An evolutionarily conserved group of proteins involved in the regulation of a large group of developmental (and other) genes.

Cajal bodies

Nuclear bodies 0.3–1 µm in size that contain RNAs and proteins and are involved in RNA metabolism-related processes.

PML bodies

Nuclear bodies 0.1–1 µm in size that contain many components, including the promyelocytic leukaemia protein (PML), and are frequently localized near Cajal bodies.

genome organization. Below, we discuss established and more recently developed methods in detail.

Sequencing-based techniques

The most common sequencing-based approach to assay chromatin architecture involves crosslinking of spatially proximal chromatin fragments followed by their isolation and sequencing, which is then used as a proxy to estimate contact frequency. Some sequencing-based techniques allow investigation of the chromatin conformation genome-wide (non-enrichment methods), whereas others depend on isolation and identification of a subset of contacts (enrichment methods). Another important distinction is between methods based on ligation of formaldehyde crosslinked chromatin fragments (C-based) and methods that do not involve ligation of crosslinked fragments (non-C-based).

Non-enrichment methods

Non-enrichment methods assay chromatin conformation at once across entire genomes. The first techniques used ligation to retain together spatially proximal fragments prior to their isolation and sequencing. Subsequently, ligation-free techniques have been developed as well. Both types of approaches capture the majority of 3D features, but they do not deliver identical information due to their inherent technical differences.

C-based methods: Hi-C and Micro-C. Hi-C is frequently used to identify 3D chromatin contacts genome-wide^{27,85} (FIG. 2). The original Hi-C protocol included dilution

during proximity ligation, a step introduced originally in 3C and 4C in order to favour ligation of intramolecular chromatin contacts to reduce artefacts. However, this dilution was not very effective, as it was shown that around 60% of contacts originate from inter-chromosomal interactions^{85–87}. This problem was circumvented by the omission of SDS treatment just before ligation, which allowed permeabilization of the nuclear membrane and, thus, chromatin digestion and ligation *in situ*^{85,86}. This modification is justified by the fact that ligation occurs in fixed nuclei, where molecular diffusion is virtually absent, and by the fact that the crosslinking reaction occurs between reactive moieties that are located in the nanometre range. Therefore, *in situ* ligation enabled a more efficient capture of true contacts, thereby delivering higher resolution for the same sequencing depth. After this methodological improvement, the omission of SDS treatment was adopted in virtually all subsequent C-based techniques. *In situ* chromatin processing allowed further development of single-cell Hi-C, which was the first sequencing-based single-cell chromatin analysis technique to be successfully established⁸⁷.

Although Hi-C is suitable for the detection of compartments and TADs, its resolution is intrinsically linked with the use of restriction enzymes and the sequencing depth. Therefore, even if Hi-C libraries are sequenced by the billions of reads, the unbiased detection of local interactions, such as enhancer–promoter contacts in the sub-TAD range, largely depends on the distribution of restriction sites, which in turn depends on the underlying sequence composition and, thus, is not uniform across the genome. This issue was first addressed concomitantly in two techniques, DNase Hi-C and Micro-C, both based on chromatin fragmentation without using restriction enzymes^{88–91}. Micro-C introduced double crosslinking and replaced the restriction enzymes used in Hi-C with micrococcal nuclease digestion^{91–94} (FIG. 2). This produces a fairly uniform fragmentation down to the nucleosome level, which increases local resolution. In addition, Micro-C (and theoretically DNase Hi-C) also retains information on nucleosome positioning, which can be jointly analysed with chromatin contact information from a single data set. However, although this technique is a promising improvement for the study of local chromatin topology, according to a recent preprint article it is less efficient in capturing long-distance and inter-chromosomal contacts compared with Hi-C⁹⁵. Therefore, careful framing of the research questions is needed to accurately select between different non-enrichment methods.

Non-C-based methods: SPRITE and GAM. Although C-based methods have been extremely successful, they have intrinsic limitations and potential sources of bias. First, like many other chromatin analysis methods, they rely on mild formaldehyde crosslinking, which is powerful but potentially limited in capturing interactions of proteins with short residence time on chromatin or containing a low fraction of amino acids that can be crosslinked^{96,97}. Second, these methods require ligation of genomic fragments prior to sequencing, a procedure

Box 2 | Manipulation of genome architecture

A fundamental question that has been very difficult to address in the past is whether genome architecture changes that are detected in different cellular conditions are a cause or a consequence of changes in gene expression^{65,230}. Use of Hi-C in *Drosophila melanogaster* lines that carry a set of known genomic alterations has allowed this question to be addressed. Intriguingly, genome topology changes stemming from chromosomal inversions or other mutations can be buffered to a large extent, such that gene expression remains robust in most, although not all, genes²³¹. Whereas this analysis used pre-existing mutant lines, CRISPR–Cas technology has also been used extensively to manipulate genome architecture. Inducing specific mutations at critical genome architecture regulatory regions has shown that genome organization into topologically associating domains with specific boundaries contributes to correct cell-type and tissue-specific gene regulation^{213,232}. In *D. melanogaster*, the deletion of specific chromatin loop anchor sequences or the insertion of boundary elements that prevent loop formation showed that Polycomb-dependent genomic loops can contribute to gene silencing during development²³³. The same approach showed that CCCTC-binding factor (CTCF)-binding sites are required for correct insulation of gene expression and that their deletion activates an oncogenic gene-expression programme²³⁴.

CRISPR–Cas was used not only to edit the genome but also the epigenome, as in the case of using a fusion of nuclease-dead Cas9 (dCas9) with DNA (cytosine-5)-methyltransferase 3A, which targets DNA methylation to specific regions and displaces CTCF binding²³⁵. Another powerful experimental tool combines CRISPR–Cas with optogenetics to induce chromatin looping upon stimulation with blue light and study its functional consequence²³⁶. Finally, the CRISPR–genome organization (CRISPR-GO) system enables inducible and reversible repositioning of dCas9-targeted genomic regions in the nucleus; CRISPR-GO was shown to reposition a locus of interest to the nuclear lamina, thereby perturbing its function, and to Cajal bodies and PML bodies²³⁷. This system could be used to target loci to other nuclear compartments in order to study the functional consequences of their relocation. Combined with the many experimental tools that enable measuring the effects of perturbation of genome structure and function, these techniques will be crucial for differentiating between cause and consequence of 3D genome organization and gene regulation.

that is only partially efficient. Third, they depend on short paired-end sequencing, which provides information only on bipartite interactions, whereas multipartite interactions in vivo chromatin interactions escape the analysis.

Several methods that do not rely on ligation of chromatin fragments allow the detection of dual or multiple interactions. In SPRITE, crosslinked nuclei are isolated and fragmented, and then individual crosslinked pieces

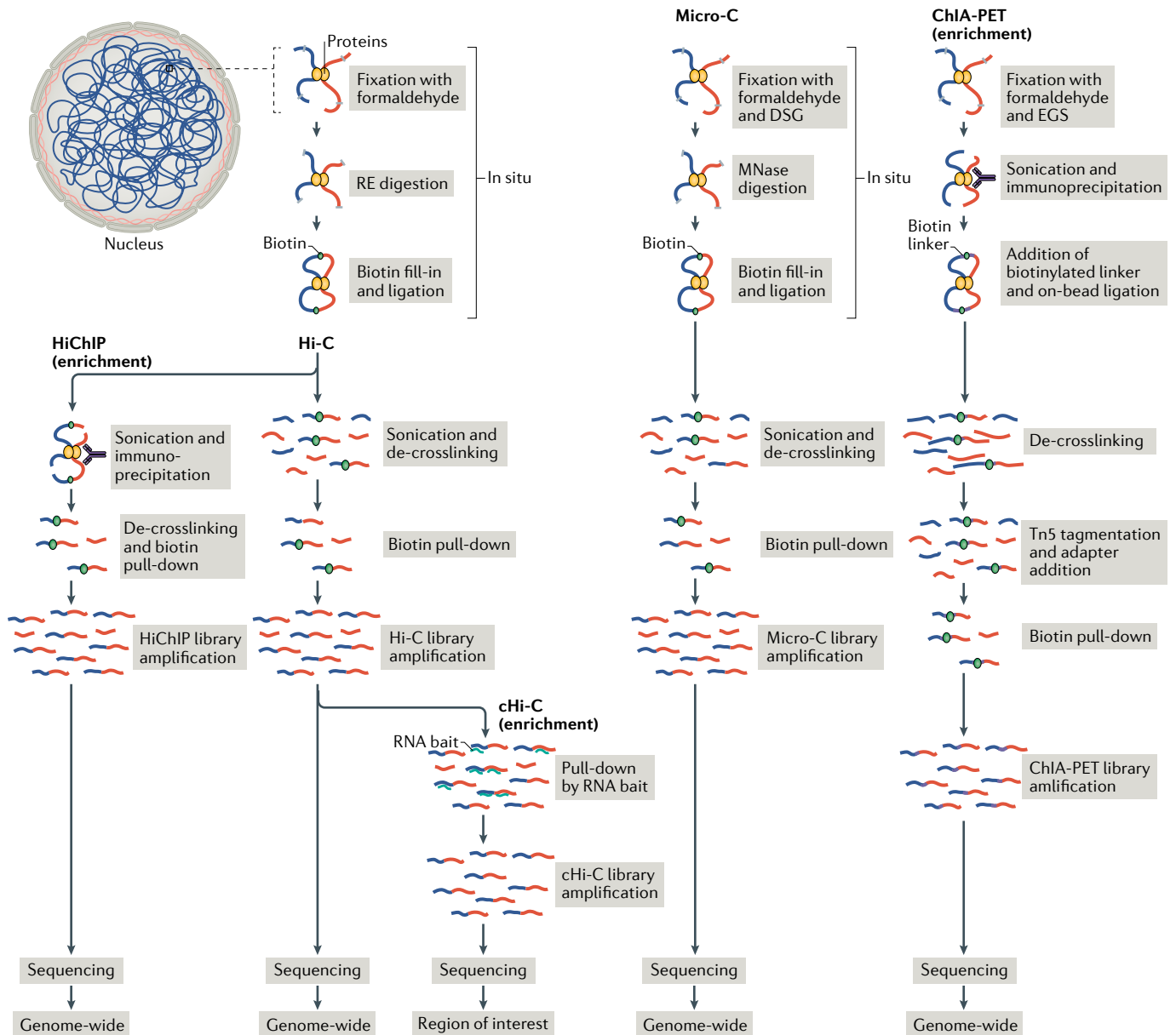


Fig. 2 | Main C-based methods for interrogation of 3D genome organization. For the application of every chromosome conformation capture-based (C-based) method, chromatin must first be crosslinked, either with one crosslinker (in most methods) or with two crosslinkers in the case of micrococcal nuclease chromosome conformation assay (Micro-C) and chromatin interaction analysis by paired-end tag sequencing (ChIA-PET)^{85,91,102}. Hi-C derivatives then use digestion by restriction enzymes (RE) to fragment the chromatin, fill in fragment ends with biotin and perform ligation, all in situ. The sample is then sonicated, de-crosslinked and enriched for informative fragments through biotin pull-down; the resulting chromatin-fragments library is subjected to amplification and sequencing⁸⁵. Hi-C chromatin immunoprecipitation (HiChIP) differs from this standard protocol by introducing an immunoprecipitation (enrichment) step just after ligation, whereas capture Hi-C (cHi-C) includes an enrichment step involving hybridization to RNA baits that represent a genomic region of interest, followed by pull-down that is performed on the final Hi-C library^{26,32}. The resulting libraries will therefore be enriched either for all

genomic contacts (in the case of Hi-C), for chromatin contacts at genomic regions where the protein of interest binds (HiChIP) or for contacts at a specific region of interest (cHi-C). Micro-C follows an almost identical procedure to Hi-C, with distinctions in the steps of fixation and of digestion, in which the restriction enzymes used in the Hi-C protocol are replaced with micrococcal nuclease (MNase)-mediated chromatin fragmentation⁹¹. This digestion modification results in a more uniform fragmentation of the genome, thereby allowing Micro-C to achieve higher resolution of local contacts. ChIA-PET provides similar information to HiChIP, but in ChIA-PET immunoprecipitation is performed immediately after fixation and sonication; and while the sample is still on the pull-down beads, a linker with biotin is added and ligation is performed on beads in order to reduce the amount of random ligation products¹⁰². Concomitant with adapter addition, the sample is de-crosslinked and fragmented using a transposase (Tn5). Finally, the sample is enriched for informative fragments through biotin pull-down and undergoes library amplification and sequencing. DSG, disuccinimidyl glutarate; EGS, ethylene glycol bis(succinimidyl succinate).

of chromatin are uniquely barcoded using multiple cycles of a split-and-pool strategy; after high-throughput sequencing, reads carrying the same combination of barcodes represent genomic sites that are a part of the same crosslinked cluster (FIG. 3). As the method does not select for specific sequence sizes, it yields bipartite as well as multipartite contacts. SPRITE has been further adapted to facilitate the capture of DNA–DNA, RNA–DNA and RNA–RNA interactions, thereby allowing to determine whether RNAs of interest are associated with a subset of genome interactions and what the relationship of the RNA is to nuclear landmarks³⁷. Finally, a single-cell version of SPRITE allows the study of multiway contacts in individual cells³⁶. Future work applying this method to a broad range of cell types and

analysing two-way and multiway contacts to a deeper level is required in order to fully exploit its advantages and appreciate its limitations⁵². GAM is an orthogonal method that can also provide frequencies of multi-valent interactions³⁵. In GAM, fixed cells are embedded in sucrose, frozen and cryo-sectioned, and the DNA is extracted and sequenced from each section^{41,98} (FIG. 3). Loci that are closer to each other in the nuclear space are co-sequenced more frequently than distant loci. As sections are taken from multiple nuclei sliced at random orientations, the co-segregation of all possible pairs of loci among a large collection of nuclear section profiles is used to generate a matrix of inferred locus proximities. GAM matrices produce maps similar to Hi-C maps but require fewer cells — a few hundred nuclei produce

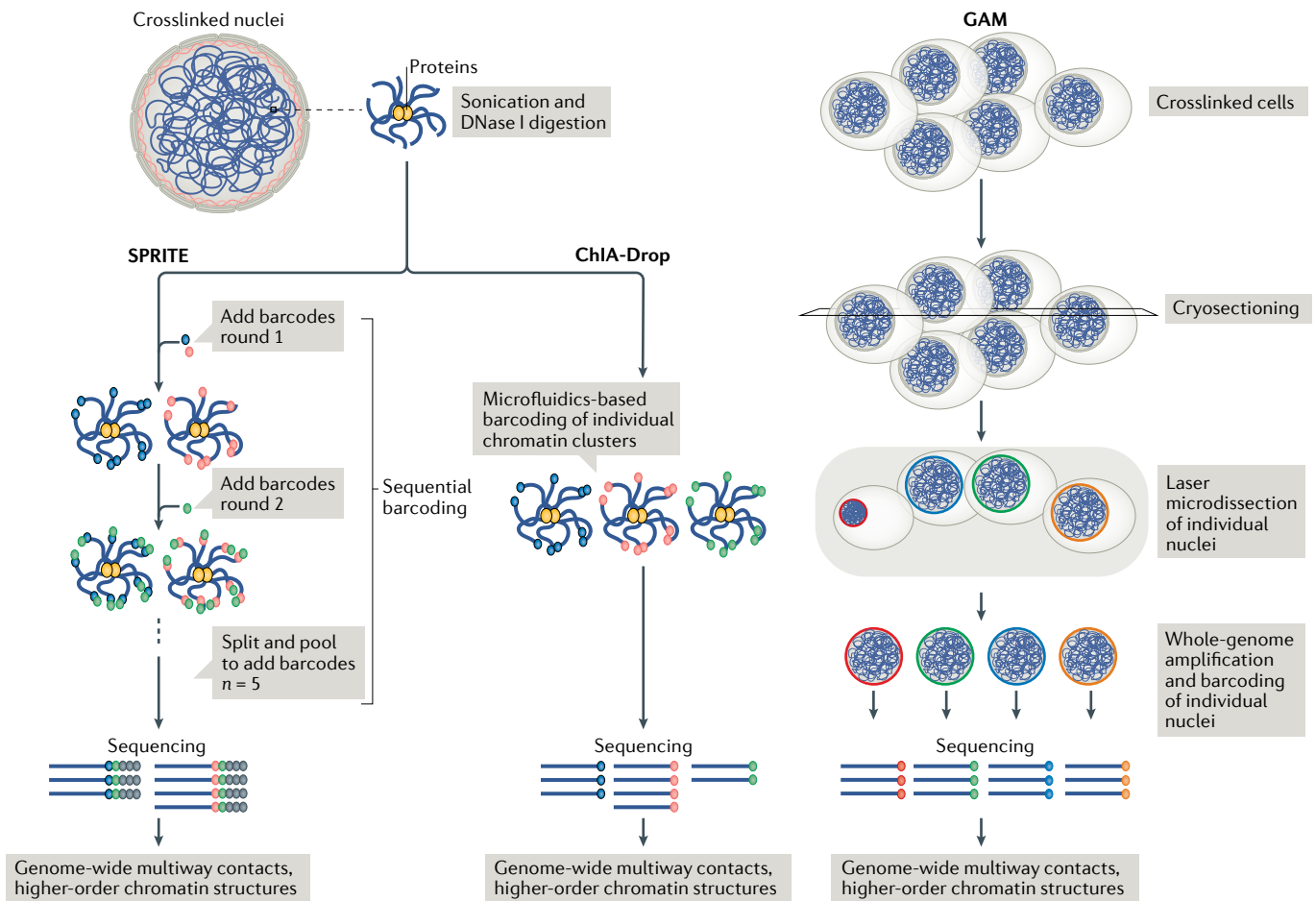


Fig. 3 | Main ligation-independent methods for interrogation of 3D genome organization. Ligation-independent methods have been developed in order to study multiway contacts that are inaccessible to ligation-based methods. The most common ligation-independent techniques are split-pool recognition of interactions by tag extension (SPRITE), chromatin-interaction analysis via droplet-based and barcode-linked sequencing (ChIA-Drop) and genome architecture mapping (GAM)^{35,41,192}. In all three, nuclei are fixed. SPRITE and ChIA-Drop then proceed with sonication and chromatin digestion by DNase I. From this point on, the two techniques take advantage of different approaches to retaining information on multiway contacts. SPRITE utilizes a split-and-pool strategy, in which every sample is split, barcoded and pooled together five times. This results in unique barcoding of all fragments that crosslinked together and, thus, to the identification of DNA sequences

that were involved in the same multiway contacts³⁵. ChIA-Drop uses microfluidics to produce a droplet carrying a unique barcode, adapters and material for DNA amplification reactions used to label a single chromatin-interaction knot, thereby allowing identification of all DNA sequences that have been crosslinked together. GAM utilizes a completely different strategy to assay genome architecture and is suitable for investigating multiway contacts, higher-order chromatin structures as well as more local contacts. In GAM, the fixed sample is embedded in sucrose and cryo-sectioned to obtain thin slices, from which individual nuclear slices are laser micro-dissected. Genomic DNA is then extracted from a single-nucleus slice followed by whole-genome amplification and sequencing. The data obtained from the different sections of a nucleus are pulled together and interactions are identified as DNA sequences that co-segregate more often than others.

maps that approximate those obtained from large populations of cells in Hi-C. Like SPRITE, GAM can identify multiple interactions, thereby enabling the direct study of multivalent enhancer–promoter interactions and of higher-order chromatin structures.

Enrichment methods

The above-described techniques detect chromatin contacts present in the nucleus irrespective of genomic location, nuclear topography or the underlying protein binding. Yet to fine-scale map chromatin folding and understand some of its functional aspects, it is necessary to detect specific contacts using enrichment approaches, thereby amplifying the contact's signal in a specific genomic region of interest (Capture-C, capture Hi-C (cHi-C)) or for a specific protein of interest (ChIA-PET, ChIP-loop, HiChIP, PLAC-seq, DamID, DamC, TSA-seq)^{21–26,30,32–34,38,39,42,99–101} (FIG. 2).

C-based methods: HiChIP, Capture-C and cHi-C. The first C-based enrichment-dependent techniques to be developed combined proximity ligation with ChIP, for example the low-throughput ChIP-loop and later, with higher throughput, ChIA-PET, which was subsequently improved to allow for more efficient mapping and detection of single-nucleotide polymorphism^{30,31,102}. However, proximity ligation in these techniques was performed in non-optimal conditions, with ChIP and sonication carried out preceding ligation, possibly affecting the accuracy of captured interactomes. These shortcomings were addressed in the next generation of protein-enrichment C-based techniques, HiChIP and PLAC-seq, in which the C-based technique is performed first and in situ, thereby creating an optimal environment for proximity ligation, followed by protein enrichment^{32,33,102}. HiChIP and PLAC-seq allow the identification of a subset of interactions forming in association with specific protein binding, but can only be used as a proxy, not definitive proof, that a protein of interest mediates the captured chromatin contacts. In addition to protein-mediated enrichment, chromatin contacts can also be enriched for a specific genomic location(s) using techniques such as Capture-C and cHi-C^{21–26} (FIG. 2). In these techniques, a Hi-C library is first generated and then hybridized to specifically designed baits (RNA or DNA) corresponding to either one large region (several megabases) of interest in the case of cHi-C or to multiple specific sites in the genome (for example, a collection of specific gene promoters) in the case of Capture-C. This allows mapping of contacts in fine detail, which would normally require 20–50-fold more sequencing without enrichment^{26,76,103}. In the future, capture approaches could be combined with other techniques to adjust them for specific needs.

Non-C-based methods: TSA and DamID. Ligation-independent techniques such as TSA-seq and DamID can also enrich for contacts associated with specific proteins and map the nuclear topology^{34,38,39,42,100}. TSA-seq relies on TSA^{34,42}. Cells are first crosslinked, followed by staining with a primary antibody against a protein of interest and, then, with a horseradish peroxidase (HRP)-conjugated secondary antibody^{34,42}. HRP

catalyses the formation of tyramide–biotin free radicals, which diffuse and covalently link to nearby proteins, DNA and RNA. The biotin moiety can be used to stain nuclei as well as to purify and sequence the associated DNA. As the amount of tyramide–biotin signal decreases with increasing distance from the antibody localization source, TSA-seq read frequencies can be transformed into 3D distances from nuclear landmarks of interest upon appropriate calibration. A second and orthogonal, crosslinking-independent technique is DamID, which involves tethering *Escherichia coli* DNA adenine methyltransferase (Dam) to a chromatin protein; the Dam moiety methylates adenines at GATC consensus DNA sites surrounding the chromatin protein of interest³⁸. Application of DamID to proteins with distinct nuclear compartmentalization allows identifying genomic domains associated with nuclear landmarks, such as the lamina-associated domains⁴⁰. More recent applications of DamID also enable identifying lamina-associated domains in single cells and, simultaneously, quantifying protein–DNA contacts and RNA expression in the same cell^{100,104}. Similar to DamID, DamC has been established as a crosslinking and ligation-free technique that can replace 4C; in DamC, a fusion protein of Dam and reverse tetracycline receptor (rTetR) is recruited to Tet operator sequences (TetOs) ectopically inserted at a genomic site of interest¹⁰¹. Methylated DNA is then detected by high-throughput sequencing, and scoring of the methylated Dam target sites around the TetOs allows quantifying chromatin contacts. DamC may be of great interest for low cell number or tissue-specific applications.

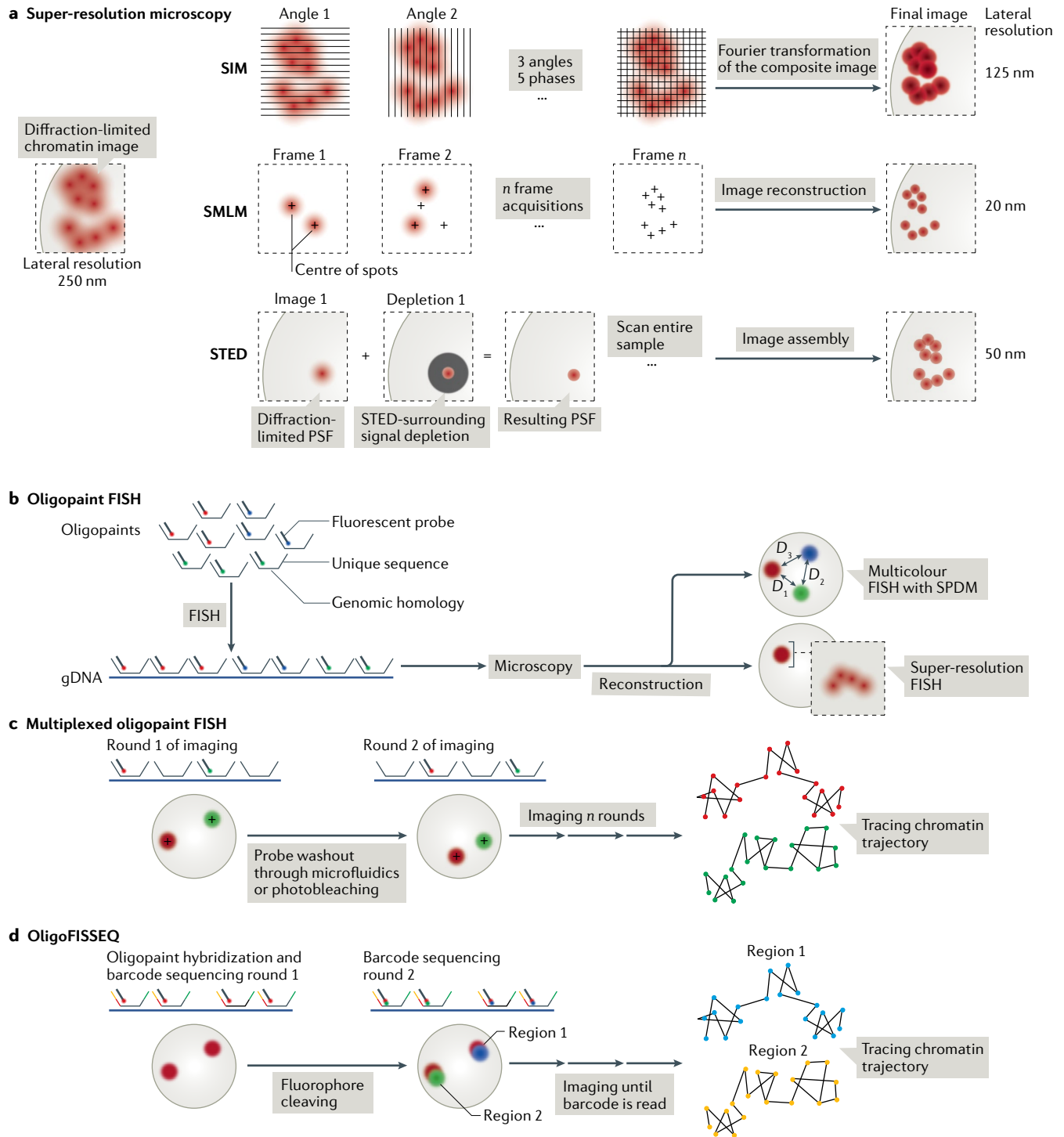
Super-resolution microscopy methods

In DNA FISH, DNA probes are hybridized to cognate genomic regions of interest and visualized by fluorescence microscopy, which allows measuring localization, shape and inter-probe distances^{4–6}. However, the study of chromosome conformation and of individual chromatin contacts under the microscope has been limited by the low number of loci that can be probed simultaneously owing to the low number of available independent fluorescence channels, and by the limited spatial resolution of traditional light microscopes. These limitations have been removed thanks to major technological advancements in light microscopy applications.

Light emitted by any point source is diffracted such that the point will appear in an image as a so-called airy diffraction pattern, the size of which is proportional to the wavelength. In practice, this property of light, together with aberrations of optical systems and light scattering, limits the resolution (the minimal distance at which two signals can be distinguished), following a formula derived by the physicist Ernst Abbe, to approximately 250 nm in the *x* and *y* axes (lateral resolution) and 600 nm in the *z* axis (axial resolution), even when using the best confocal microscopes and image processing software. For decades, the resolution of light microscopy was believed to be intrinsically limited by diffraction, but imaging technologies have progressed at a remarkable speed, allowing the detection of increasing numbers of nuclear components at a spatial resolution surpassing

Lamina-associated domains
Chromosome domains associated with the nuclear lamina in the 3D nuclear space.

Airy diffraction pattern
A diffused circle surrounded by rings of decreasing intensity generated when a laser passes through a circular opening.



the Abbe limit. These methods, collectively called super-resolution microscopy, increase spatial resolution mainly in three different ways, and here we discuss their applications in 3D genome organization research (FIG. 4a). Detailed descriptions of these methods can be found in more specialized microscopy reviews^{105,106}.

Structured illumination microscopy (SIM) is an approach to super-resolution microscopy that increases resolution by a factor of two in each axis by exploiting a non-uniform illumination pattern: the sample is serially exposed to light from different angles and

different axial phases^{107–109} (FIG. 4a). This illumination pattern interferes with the sample in a manner that can be conveniently analysed in the Fourier mathematical space to improve resolution. Despite its complexity, the advent of commercially available SIM microscopes and software and the fact that the technology is compatible with standard fluorophores, labelling procedures and multicolour imaging have stimulated the widespread application of SIM. SIM has allowed assessing the unprecedented details of chromatin and nuclear organization, such as the relations between chromatin

◀ Fig. 4 | **Microscopy and FISH-based methods for 3D genome investigation.**

a | Super-resolution microscopy techniques overcome the diffraction limit using different approaches. In structured illumination microscopy (SIM), the sample is exposed to a series of non-uniform illumination from different angles and axial phases^{107–109}. The resulting light pattern is analysed by Fourier transformation to achieve a final mathematical reconstruction of the image, which improves lateral and axial resolution by twofold. Single-molecule localization microscopy (SMLM) uses low excitation energy that causes a stochastic excitation of photo-switchable fluorophores for precise localization of the centre of emission^{112–115}. Sequential images of the sample are taken, in which fluorophores turn either bright or dark, and the final image is created by a superposition of all imaging cycles. In most practical applications, this method yields a lateral resolution of up to 20 nm. Stimulated emission depletion (STED) uses stimulated emission depletion through the combination of two lasers: an excitation laser illuminates the sample in the middle and a doughnut-shaped depletion beam depletes the surrounding signal^{118,119}. In practice, STED reaches lateral resolution of about 50 nm and axial resolution of about 80–600 nm. **b** | Oligopaints are fluorescently labelled synthetic DNA oligonucleotides that can be combined with fluorescence in situ hybridization (FISH) to label, visualize and measure the distances between genomic regions¹²². **c** | Oligopaints can be further modified to allow sequential imaging by incorporating sample bleaching or automatized microfluidics with microscopy. Following every round of imaging, the oligonucleotides are washed out before proceeding with a new round of hybridization and imaging^{44–48,123}. Distant genomic regions are imaged simultaneously using different detection fluorophores whereas their neighbouring regions are imaged in the next round, thereby allowing chromatin tracing. **d** | In oligo fluorescence in situ sequencing (OligoFISSEQ), oligonucleotides contain barcodes that can be read through hybridization with a set of specific primers, to which fluorescently labelled dinucleotides are ligated. The fluorescent signal is then imaged and cleaved off. This process is repeated until the barcode is read in full (inferred from the specific combination of fluorophores)^{14,15,219}. gDNA, genomic DNA; PSF, point spread function; SPDM, spectral position determination microscopy.

and the nuclear periphery or the physical structure of TADs in single cells^{13,53,110}. In particular, the analysis of mammalian TADs using SIM has revealed that TADs are subdivided into the smaller CNDs: as CND boundaries vary from cell to cell, ensemble Hi-C experiments blur their identification, thereby illustrating the power of single-cell, super-resolution imaging to illuminate 3D genome organization features that are inaccessible to cell population-based technologies^{57,111}.

A second family of super-resolution microscopy methods is called single-molecule localization microscopy (SMLM), which includes stochastic optical reconstruction microscopy (STORM), photo-activated localization microscopy (PALM) and fluorescence photo-activated localization microscopy (FPALM)^{112–114}. All three methods use fluorophores that can be converted from a fluorescent (or activated) state to a dark (or inactivated) state (and vice versa) and rely on the stochastic excitation and detection of spatially separated single fluorophores. The spatial separation is achieved by making sure that only a small fraction of the total population of fluorophores in the sample can emit light, so that individual emitters do not overlap in a single imaging frame¹¹⁵. Sequential imaging using cycles of activation and inactivation of the fluorophores, followed by the precise localization of the centre of emission of the individual fluorophores and the superposition of all imaging cycles, generates super-resolution images that can reach a lateral resolution of 20 nm in biological samples (3D images can be obtained using various methods)¹¹⁵ (FIG. 4a). The application of these methods has provided crucial insights into the fundamental folding of chromatin in the nucleus. Nucleosomes were shown to transiently interact to form clutches of various sizes

interspersed with nucleosome-depleted regions¹¹⁶. At a higher scale of organization, nucleosomes were found to form CNDs, that is, aggregates with a diameter of ~160 nm, within which individual nucleosomes display highly correlated motion in live cells¹¹⁷. This organization suggests that CNDs may arise from coordinated behaviour that might reflect multiple, dynamic nucleosome interactions, consistent with recent analysis of fixed chromatin by SIM^{57,111}. It will be interesting to study whether CNDs might regulate genome functions such as gene expression (in particular, the frequency of enhancer–promoter contacts) or DNA replication.

The third approach to super-resolution microscopy is stimulated emission depletion (STED). This technique uses a configuration similar to confocal microscopy but with an additional laser called the depletion beam, which illuminates the sample in a doughnut shape that has zero intensity at the centre of the excitation laser^{118,119}. This illumination provokes the depletion of emissions in the periphery and only allows emission in the centre, thereby generating a sub-diffractive point spread function. In most applications, STED reaches a lateral resolution of 30–50 nm and high axial resolution can also be obtained (FIG. 4a). The drawbacks of this method are its strong laser intensity and the requirement for specific fluorophores. A modified version called reversible saturable optical fluorescence transitions (RESOLFT) allows using lower beam intensities¹²⁰. Importantly, SMLM and STED do not have a theoretical resolution limit and a combination of the two methods has achieved axial and lateral resolutions below 3 nm in cells¹²¹. Therefore, imaging applications are quickly enabling investigation of chromatin and nuclear architecture at the macromolecular scale.

A remaining limitation of these super-resolution microscopy methods is throughput, as they are limited to using two or three colours, which restricts the number of loci that can be analysed simultaneously. Recently, however, oligonucleotide-based FISH protocols called oligopaints were coupled with microfluidics to allow multiple cycles of hybridization¹²² (FIG. 4b,c). This conjunction of methods enabled sequential probe hybridization and assaying multiple different loci with high precision in the 3D nuclear space^{12,15,44–48,123}. These techniques allowed obtaining distance distribution maps among all imaged points that recapitulate the maps obtained from Hi-C experiments and provide 3D trajectories of chromatin molecules at high resolution and in thousands of cells, something that is unattainable even in single-cell Hi-C (FIG. 4c,d). These techniques include multiplex FISH imaging, which helps establish high-resolution tracing of chromatin folding of megabase-size genomic domains by labelling several tens of locations in the genome simultaneously^{44,46,48,123}; optical reconstruction of chromatin architecture (ORCA)⁴⁷; Hi-M⁴⁵, which is a multiplexed, sequential imaging approach; and oligopaint fluorescence in situ sequencing (OligoFISSEQ)¹⁴ (FIG. 4b–d). Importantly, OligoFISSEQ is a method that combines hybridization of barcoded oligopaints with in situ sequencing technology, which is used to read out the barcode carried by the oligos (FIG. 4d). This combination makes OligoFISSEQ a powerful high-multiplexing technology¹⁴. In situ sequencing can also be coupled

Point spread function

The response of an imaging system to a point object. If the object is below the microscope resolution, it will appear larger than it really is.

Sub-diffractive point spread function

A point spread function of smaller size than that generated by diffraction-limited systems.

with Tn5 transposase-mediated random insertion of DNA-sequencing adapters into hundreds of positions of fixed genomic DNA. In situ amplification can then be used to insert unique molecular identifiers that are sequenced in situ prior to ex situ sequencing in order to identify the genomic region of Tn5 insertion. This approach allows mapping the 3D location of hundreds of loci per cell, and is a powerful alternative to hybridization-based imaging methods¹⁶.

Currently, it is possible to simultaneously visualize thousands of DNA loci, hundreds of different RNA molecules and several proteins or histone modifications, thereby enabling high-throughput structure–function analyses in thousands of single cells and truly inaugurating the field of spatial imaging-based 3D genomics^{12,15}. These light microscopy methods are accompanied by developments in electron microscopy, with electron microscopy tomography allowing the study of chromatin at nanometre resolution¹²⁴. Each of these methods has advantages and limitations. For instance, methods with very high spatial resolution are typically not optimal for the description of architectures of large domains owing to a slow acquisition process and to the intrinsic noise in the images that are obtained. However, advanced OligoSTORM imaging provides powerful information on 3D genome organization that is complementary to molecular techniques such as Hi-C, thereby enabling the investigation of genome architecture and function to a degree that was unthinkable a decade ago¹⁴.

Computational analysis and modelling

Although the methods discussed above provide important insights into 3D genome organization and function, they are still limited in their ability to describe how the chromatin fibre folds in the 3D space of the nucleus and they cannot predict structural changes that would result from perturbations such as mutations in genes or in gene-regulatory components. Evaluating the impact of architecture on genome function remains even more inaccessible at present. All of these limitations have stimulated computational analyses and the development of mathematical modelling that, in conjunction with experiments, might help achieve a quantitative and predictive understanding of chromosome architecture and function.

Analysis of Hi-C data

The advent of Hi-C and related technologies has raised strong interest in the development of matching computational analysis tools, owing to the inherent complexity of Hi-C data. The achievable spatial resolution of Hi-C is affected by sequencing depth, library complexity and the DNA-cutting frequency of the enzyme used for chromatin fragmentation. As the number of possible chromatin fragment interactions is extremely high ($>10^{14}$ in the human genome, when using 4-base cutter restriction enzymes) and the sequencing depth of a typical experiment is limited, Hi-C matrices are sparse, that is, many entries in the matrices are 0, if they are not represented at the appropriate resolution. This makes it impossible to distinguish between genuine absence of contacts and absence of contacts owing to low sequencing depth. Furthermore, the

different sizes of restriction fragments across the genome, differences in mappability between regions with high or low density of repetitive elements and the decay of interaction frequencies with an increase in genomic distance make Hi-C matrices typically very heterogeneous in terms of contacts at different genomic locations or across different distances. All of these factors limit the resolution with which one can call contact regions or domain boundaries, and generate difficulties in defining the precise locations of compartments, TADs and chromatin loops. The first Hi-C study²⁷, which used a 6-base cutter and achieved low sequencing depth, produced reliable matrices at a resolution of 100 kb and identified the compartments. To this end, Hi-C matrices were normalized by genomic distance, converted to correlation matrices and subjected to principal component analysis, which distinguished the active (A) and inactive (B) compartment types. Later algorithms additionally applied clustering steps such as Gaussian hidden Markov modelling to Hi-C maps based on much deeper sequencing, leading to further specification of epigenetic compartment signatures and more detailed stratification of the A compartment into two sub-compartments and the B compartment into three sub-compartments^{85,125–129}.

The computational identification of TADs required high-resolution maps, which were published 3 years after the publication of the first low-resolution Hi-C experiment^{53–55,130}. Although nowadays TAD calling is done routinely, there is no clear consensus method but rather numerous TAD callers that are based on different principles. Initial computational approaches such as the insulation score and the directionality index determined TAD boundaries by defining a 1D linear score of a bin-fractionated genome, where the bin of the local minima (for the insulation score) or the bin between local minima and maxima (for the directionality index) would determine the boundary position^{55,131,132}. These approaches, however, could not inform on TAD hierarchy and missed identifying nested TADs. Subsequently, other computational approaches were developed to address this issue either by further developing the linear score approach (Matryoshka)¹³³, by clustering contacts' map data (ICFinder¹³⁴, TADpole¹³⁵) or by using graph theory-based algorithms that identify nested TADs as contact subnetworks connecting to form larger TADs (3DnetMod)¹³⁶. Furthermore, numerous other computational tools have been developed that combine these approaches with different efficiencies at different scales and resolutions^{137–140}.

The third major feature of Hi-C data are chromatin contacts and loops, which, like TADs, became detectable as the data became more resolute. Specific chromatin contacts are defined as statistically significant increases in contact detection in comparison with a general background model. This is the basis of Fit-Hi-C, a computational tool that assigns a statistical confidence to a contact by using random polymer modelling while accounting for known Hi-C biases such as genomic distance; an adapted version, HiC-DC, additionally accounts for sparsity and overdispersion and yields a more conservative statistical significance estimate^{141,142}. However, a locally enriched contact — a chromatin

loop — might elude algorithms that use only a general background model to estimate statistical significance of enrichment. HiCCUPS, one of the first loop-dedicated algorithms, identifies a chromatin loop as the most enriched bin in comparison with its immediate neighbourhood while using high-resolution 5-kb Hi-C data as an input⁸⁵. This algorithm helped drive the discovery of a specific subtype of loops, CTCF loops, and contributed to the development of the loop-extrusion model, thereby demonstrating the importance of specialized algorithm development in order to grasp the full biological significance of the experimental data. In-depth reviews and websites have compiled and compared available compartment, TAD and loop callers^{139,143–147}. The increasing robustness of primary computational tools to identify 3D genome features has led to a blooming of applications aimed to identify DNA sequences of biological significance linked with genomic regions in spatial proximity as mapped by Hi-C techniques. These applications have enabled associating genes with putative enhancers based on contact frequency, epigenomic and DNA features; identifying novel regulatory elements from genome-wide association studies; and assigning a potential role for short tandem repeats in genome organization^{148–155}.

Although these computational tools can provide precious information on genome structure and function, the cost of obtaining high-resolution Hi-C maps can become prohibitive, particularly when many experimental conditions need to be compared. In order to tackle this problem, a machine learning approach based on deep convolutional neural networks has been used to impute higher-coverage Hi-C maps from low-coverage data in order to increase the resolution with which loops or TAD borders can be defined¹⁵⁶. This function is important in order to identify genomic features that might be involved in the regulation of these structures even if the data are not sufficiently resolute.

3D chromatin modelling

The computational tools discussed above provide new information about regulatory elements and their function, but they do not inform on 3D architecture. Three main types of modelling strategies have been used to infer 3D genome folding, although some methods can blur this classification as they have characteristics belonging to more than one type^{137,157–160}. The first modelling strategy is the bottom-up approach of polymer modelling, which attempts to infer and understand chromosome architecture from first principles, typically modelling chromosomes as self-avoiding polymers moving in a confined space that represents the nucleus (FIG. 5a). Applications aim to identify components regulating 3D folding, and thus they try to reduce the number of variable parameters describing the polymer behaviour while maximizing the fit between experimental data, typically Hi-C contact matrices and analogous matrices that are derived from measuring contacts in snapshots taken at given times after starting polymer motion simulations. This modelling strategy has been applied to rationalize the decay in contact frequencies between chromatin regions as a function of the linear distance

separating them^{161,162}. More recently, these models have offered an explanation for the formation of domains of active and inactive chromatin, the generation of TADs through loop extrusion and the contribution of epigenetic features such as chromatin types to the formation of TADs and compartments^{58,67,128,163–166}. The combined role of loop extrusion and of active and inactive compartments in the determination of global chromosome organization has also been studied⁶⁸. Furthermore, in addition to intra-chromosomal contact frequencies, this strategy allowed the investigation of inter-chromosomal contacts¹⁶⁷. A current limitation of these models is that they can typically reproduce and predict some, but not all, of the features of 3D chromosome folding and, in particular, they usually do not perform equally well at different scales (loops, TADs, compartments, chromosome territories)^{137,138}. This is partly due to the considerable computational time required for the iterative simulation processes that are involved in generating the models, and interesting ongoing developments involve accelerating computation¹⁶⁸.

An alternative, physics-based bottom-up modelling strategy does not aim at minimizing the number of parameters to describe polymer behaviour. Instead, it models chromosomal regions as polymers, in which each monomer represents a genomic region of fixed size and can interact with any other monomer with a specific energy. Each of the interaction energies can be adjusted until the configuration ensemble of the polymer produces a contact matrix that resembles the Hi-C data matrix. This approach allows searching for the monomers that have the most crucial role in driving the specific 3D configuration defining the genomic region of interest^{169–171}. Furthermore, it can also be used to study the 3D path of the chromatin fibre in the resulting polymer models and to compare it with 3D data such as those provided by imaging methods in order to relate contacts to 3D architectural features of the region of interest⁴³.

The second type of modelling strategy is the top-down approach of restraint modelling, starting from data that are often derived from Hi-C maps and sometimes integrated by maps of chromatin–nuclear lamina interactions, in order to infer the 3D architecture of genomic loci, entire chromosomes or the whole nucleus (FIG. 5b). In some applications, the contact maps are used to set restraints that the models must satisfy in setting the 3D folding paths of chromatin fibres. The modelling result can be a consensus genome structure or an ensemble of structures, which reflects the structural variability among cells or during time^{28,172–179}. This type of modelling can also deliver information about chromatin folding dynamics, provided Hi-C data from time course experiments are available. This is possible by interpolating the restraints through each of the time points¹⁸⁰. Another interesting data-driven modelling approach uses a population deconvolution approach, in which Hi-C data are used to generate a large population of structures that, together, reproduce the experimental interaction patterns. This approach has been extended to incorporate chromatin–lamina interaction and imaging data^{46,181,182}.

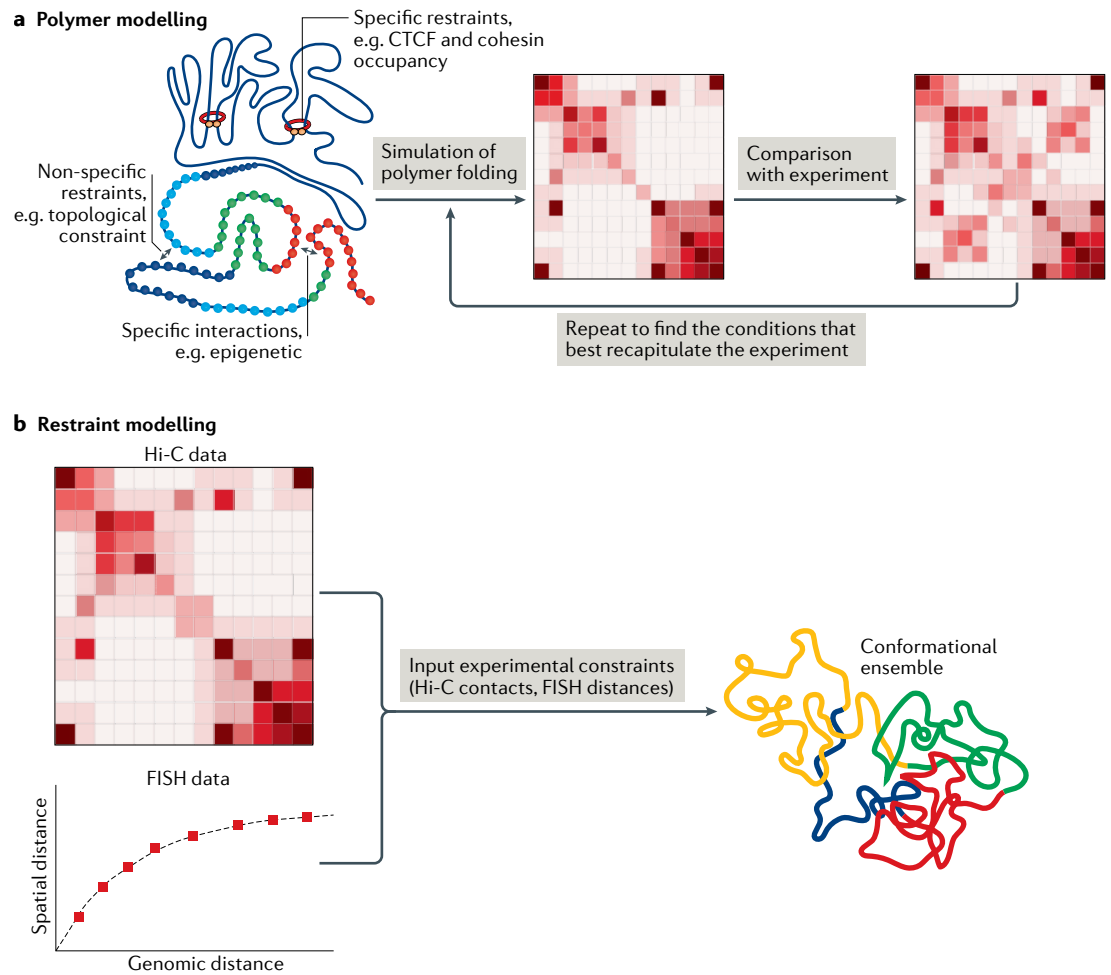


Fig. 5 | Computational modelling of the 3D genome. Two main computational strategies have been devised to investigate chromosome folding and the mechanisms driving it: a bottom-up strategy (polymer modelling) and a top-down strategy (restraint-based modelling)^{137,157,158}. **a** | Polymer modelling mimics the physical behaviour of the chromatin fibre that is represented as series of monomers (beads) on a string, and in which attraction or repulsion forces can be attributed based on first principles. The behaviour of the polymer is influenced by non-specific restraints, for example, imposing that the beads must be self-avoiding; by specific restraints, such as cohesin-dependent loop extrusion that is blocked at convergent CCCTC-binding factor (CTCF) sites; and by specific interactions, such as attraction between beads sharing the same epigenetic modifications. Such a strategy can produce virtual contact maps that can be compared with Hi-C interaction matrices. This process is reiterated until the input parameters can reconstitute a simulation that optimally recapitulates experimental maps. Polymer modelling allows to infer the mechanisms and estimate the forces that are necessary or sufficient to achieve the chromatin conformation that is most similar to the experimental data¹⁵⁹. Beads of different colours indicate regions carrying different epigenetic modifications. **b** | Restraint-based modelling uses experimental data such as Hi-C contact maps or fluorescence in situ hybridization (FISH)-measured nuclear distances to infer all of the spatial restraints necessary to determine the structure of the genomic region of interest. The resulting model is an optimally reconstructed 3D folded chromatin fibre that gives information on spatial positioning of chromatin regions.

The recent progress in computation speed led to the deployment of another cohort of 3D chromosome folding prediction tools, which are based on machine learning methods that use epigenomic and chromosome conformation information as input and display the predicted 3D architecture as output^{171,183–188}. Such computational tools rely on input data obtained from several different cell lines to train their models and identify the minimum necessary signature to accurately predict an enhancer–promoter pair, a promoter–promoter pair and CTCF loops as well as for contact quantification^{183,184,187,188}. Recently, two tools, Akita and DeepC, used convolutional neural networks to predict

3D folding solely on the basis of DNA sequence^{185,186}. These kinds of computational tools could become very important to enable making predictions from experimental samples, for which the full epigenome data sets are not available because of sample-quantity limitations, for example in the case of patient samples.

A third type of modelling strategy that combines both top-down data-driven models and bottom-up physical models has been described¹⁸⁹. This model uses parameters derived entirely from a Hi-C experiment as input, but also factors in a polymer’s energy function as in bottom-up approaches. However, in this case, the energy function is designed strictly from biological factors that have been

demonstrated to have a role in 3D genome organization, which ensures biological relevance while simultaneously allowing for mechanical investigation. With monomers 1 Mb in size, this model successfully reconstituted the radial positioning of entire chromosomes and uncovered previously unknown contributions of distinct biological processes (separation of the A and B compartments, centromere clustering, inter-chromosomal contacts). However, the large monomer size limited resolution and prevented the capture of more local features such as sub-TAD or loop structures, but the currently available computational power could allow decreasing the monomer size and testing whether mechanistic insights into more local structures can be correctly modelled.

Improved algorithms and the ever-increasing computation power will soon allow modelling the dynamics of whole-genome folding at high spatial and temporal resolution, making computational methods crucial complementary tools to the experimental methods.

Emerging genome structure technologies

Many outstanding questions remain in the research of nuclear architecture, and it is therefore not surprising that new sequencing-based methods, microscopy-based methods and computational methods are continually being developed.

One outstanding question in the field is how to address single-cell variability while not compromising high throughput. Sequencing-based techniques address this through the adaptation of C-based techniques and C-independent techniques for single cells^{36,87,190}. The first of these single-cell adaptations was single-cell Hi-C (scHi-C), which revealed high inter-cell contact and TAD variability and indicated that TADs are highly stochastic domains⁸⁷. This finding, however, put into question whether this major Hi-C feature (TADs) represents actual physical structures or reflects statistical average rather than a physical reality. Later, microscopy studies settled this controversy by showing that TADs do correspond with physical domains, but also that they have highly variable structures, clearly emphasizing the need to focus on techniques that provide information on large numbers of single cells^{43,44,57}. Indeed, an increasing number of chromatin analysis techniques are being developed into single-cell applications to address this issue and study chromatin conformation stochasticity and inter-cell variability^{36,190–193}.

Another major goal pertaining to C-based methods is to overcome the resolution limit and potential crosslinking bias. Although alternative fragmentation techniques (Micro-C, DNase-Hi-C) successfully deal with the resolution problem, every technique that relies on crosslinking is inherently biasing fragmentation towards open chromatin regions^{88,91}. A recently published method, Cap-C, approaches this problem by exchanging the standard formaldehyde crosslinking with dendrimer crosslinking. By using three differently sized molecules, Cap-C allows homogeneous crosslinking of open and closed chromatin, thereby achieving more uniform fragmentation and higher resolution^{88–91,194}. As this is a straightforward change to current C-based protocols, it has the potential to be widely implemented.

The question of how to obtain spatial coordinates of the chromatin in the nucleus in a high-throughput manner and how to integrate chromosome conformation data with the spatial position has been difficult to answer using sequencing-based techniques. Recently, two new methods to study nuclear topology and higher-order organization based on ligation-free methodology were published, genomic loci positioning by sequencing (GPSeq)¹⁹⁵ and chromatin interaction analysis by droplet-based genomic analysis (ChIA-Drop)¹⁹², which provides information on multivalent interactions (similar to SPRITE). In ChIA-Drop, crosslinked and fragmented chromatin is loaded onto a microfluidics device so that individual crosslinked molecules are partitioned into droplets that contain unique barcoding reagents (FIG. 3). After pooling, high-throughput sequencing and identification of reads carrying the same barcodes, putative 3D interactions are identified. In *Drosophila melanogaster*, ChIA-Drop was performed using fewer than 10,000 cells, and thus could be suitable for analysing rare cell types. Furthermore, the possibility to enrich for interactions that depend on specific proteins allows inferring the relative position of the interacting regions relative to nuclear bodies or landmarks¹⁹². GPSeq primarily focuses on the study of radial chromosomal positions in the nucleus by performing restriction enzyme digestion over a time course in situ, which allows the capture of the most nuclear periphery-adjacent chromatin following short-term digestion, whereas the longer digestion times capture progressively more interior parts of the genome. However, to infer distances to the periphery correctly it is necessary to perform YFISH (in which a Y-looking FISH adapter is ligated on the restriction enzyme overhang while the other side of the adapter interacts with FISH probes) coupled with super-resolution imaging over a time course. Using this approach, it is possible to investigate not only the radial position of chromosomes but also the radial positions of DNA replication, double-stranded DNA breaks and mutations¹⁹⁵. Recently, a computational method called SPIN (spatial position inference of the nuclear genome) has been developed to predict genome-wide spatial positioning in the nucleus. The method integrates spatial multi-omics data including TSA-seq, DamID and Hi-C in a computational framework based on a hidden Markov random field to localize clusters of chromatin contacts relative to nuclear bodies such as nuclear speckles or the lamina¹⁹⁶. This complementary tool of experimental and computational multi-omics methods might provide the essential missing components in the nuclear organization research toolbox.

Finally, the last outstanding questions in the field we discuss are how to achieve higher spatial resolution in microscopy and how to assay chromatin dynamics of individual genomic loci. In order to achieve spatial resolution, one has to be able to image beyond the diffraction limit. In addition to super-resolution microscopy, several recent publications have reported an alternative approach called expansion microscopy (ExM), in which the sample is embedded in a polyelectrolyte gel that expands four or five times when immersed in water^{197–199}. ExM offers imaging of structures that are beyond the

Dendrimer crosslinking

A procedure in which formaldehyde crosslinking can be followed or replaced by crosslinking with dendrimers, which are highly ordered, branched polymeric molecules of different sizes.

Diffraction limit

The points where two airy patterns are too close to be distinguishable.

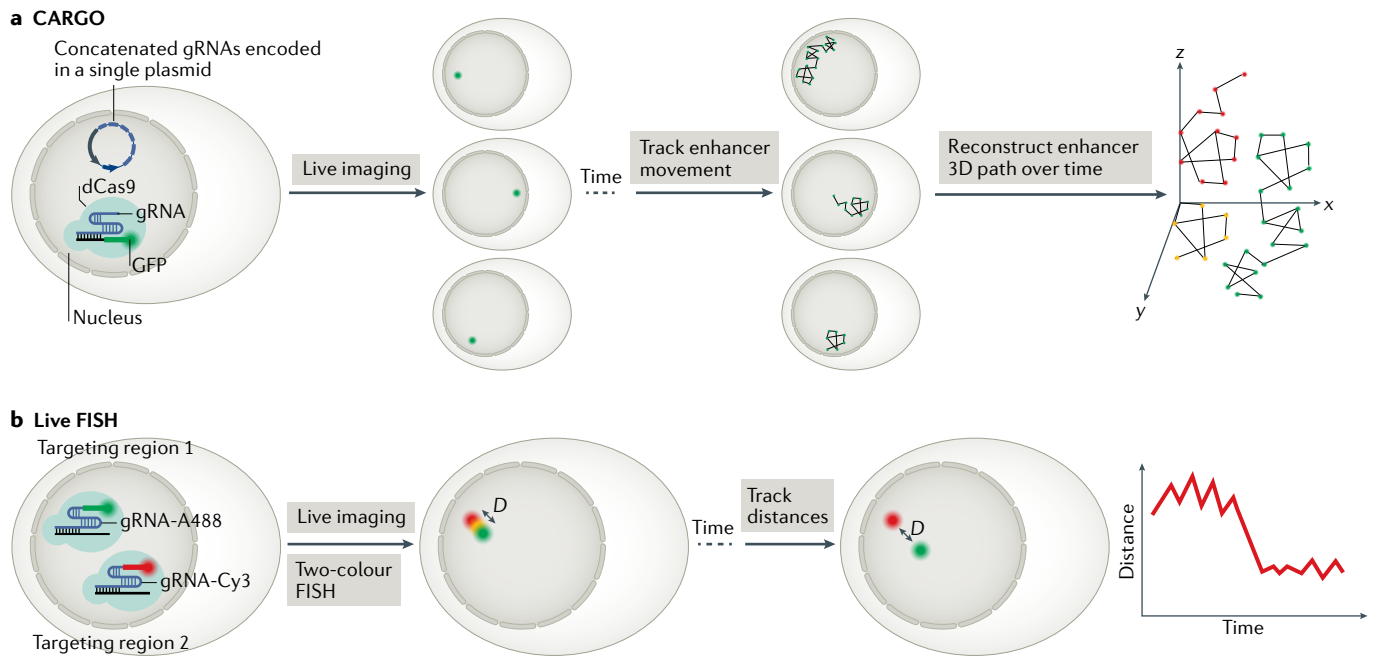


Fig. 6 | Live microscopy using CRISPR–dCas9 to study the 4D genome. Live-cell microscopy is one of the few approaches that informs on the dynamics of chromatin contacts. Multiple different methods allow the study of 4D chromatin dynamics (changes to 3D chromatin structure over time)^{50,204–207}. Here, we illustrate two such methods based on nuclease-dead Cas9 (dCas9) recruitment to the chromatin: chimeric array of gRNA oligonucleotides (CARGO) and live fluorescence in situ hybridization (FISH). **a** | CARGO utilizes a single plasmid encoding multiple guide RNAs (gRNAs) targeting the same genomic region of interest, for example an enhancer, in order to amplify the fluorescence provided by dCas9–EGFP⁴⁹. The region of interest can be imaged over time to study its spatial dynamics. **b** | Live FISH utilizes two fluorescently labelled gRNAs (one red (Cy3) and one green (A488)) targeting different regions of interest²⁰⁶. The two regions can be labelled and imaged simultaneously, which allows tracking the dynamics of the regions over time. *D*, distance.

diffraction limit using conventional microscopy, and according to a recent preprint article, when combined with super-resolution microscopy, ExM achieved resolution of 5 nm¹⁹⁸. Furthermore, ExM can be extremely powerful for spatially precise positioning of RNA species in situ and has been recently used in combination with FISSEQ technology to perform RNA in situ sequencing in an unbiased manner²⁰⁰. This technology conglomeration offers great promise for the future, as it combines different principles to achieve sub-diffractive resolution and multiplexing. One could easily imagine extending its applications to multiplex DNA FISH or in situ sequencing methods in order to analyse the traces of chromosomes, chromosome domains or individual loci at high resolution. However, it is important to keep in mind that sample expansion can alter the ultrastructure of the chromatin and it will be necessary to ensure that the structure remains preserved under standard conditions.

There are two major bottlenecks to studying chromatin contact dynamics of individual loci. First, in order to visualize such contacts, cells usually had to be subjected to heavy genome engineering to insert either lac-O or tet-O arrays^{50,201–203}. Second, the signal must be sufficiently strong in order to visualize individual loci. Multiple different methods have been developed to achieve this goal^{49,50,204–207}. Chimeric array of gRNA-oligo (CARGO) and CRISPR–Cas-mediated Live FISH are examples of two independently developed live-imaging techniques that addressed these limitations

by using the CRISPR–Cas9 system. CARGO uses multiple guide RNAs (gRNAs) targeting nuclease-dead Cas9 (dCas9)–EGFP to certain genomic locus to achieve efficient fluorescence-signal amplification and circumvent the need for strenuous genome engineering⁴⁹ (FIG. 6a). This method enabled detection of the mobility of *cis*-regulatory elements during cell differentiation in relation to their expression, and offers great promise as it is relatively simple⁴⁹. Similarly, CRISPR–Cas-mediated Live FISH utilizes dCas9 to target a region of interest but here the gRNAs are fluorescently labelled, thereby amplifying the signal more than fourfold²⁰⁶ (FIG. 6b). Furthermore, the use of catalytically active Cas9 together with dCas9 allowed the simultaneous visualization of double-stranded DNA breaks and fluorescent double-stranded DNA break-repair proteins, practically creating a live Immuno-FISH²⁰⁶. Finally, Live FISH was further expanded by coupling the dCas9–gRNAs with the dCas13–gRNA system, thereby granting visualization of both DNA and nascent RNA transcripts in live cells^{206,207}. Together, these and similar dCas9-based techniques might become valuable for studying chromatin and transcription dynamics in live cells, and open venues for application ranging from basic science to diagnostics^{50,208}.

Future directions

Genome architecture as a field of research has come a long way in a remarkably short period of time thanks to multidisciplinary that was driven by technological

advancements. In this Review, we discussed major discoveries in chromatin conformation and nuclear topology through a technical prism. However, there is still so much we do not understand and that is not accessible to us owing to methodological shortcomings.

The next decade will likely see a continued expansion of imaging-driven techniques with a strong emphasis on multiplexing and on live microscopy, especially in conjunction with sub-diffractive resolution. As we already now see the implementation of Live FISH, further development and specialization of these methods could possibly help to study enhancer–promoter dynamics with respect to transcriptional output^{206,207}. Furthermore, live microscopy-based techniques could be well suited to study the kinetics of transcription factor binding to chromatin, a subject that is poorly understood. In addition to live microscopy, the throughput of the super-resolution FISH-based methods will likely further increase and help study inter-cell variability. However, these predictions are based on the premise that the hardware necessary for these techniques will become more available and affordable.

Regarding sequencing-based methods, there is already a strong tendency to use different methods on the same sample, for example nucleosome occupancy and Hi-C (Micro-C, DNase-Hi-C) or bisulfite sequencing and Hi-C, in order to obtain different types of information from the same sample, but also to expand the amount of information that can be extracted from limited material such as patient or rare-cell samples^{91–93,191}. This trend will likely continue, and new multifaceted approaches will emerge allowing the collection of complex data. Furthermore, existing techniques are constantly being adapted to extend their applicability. For instance, two recent Hi-C-based techniques and a SIM imaging-based technique have been described that allow inspection of sister chromatid topology at the cell population level^{73,74,209}. These techniques mark a significant milestone because, unlike other sequencing-based

techniques, they allow the study of chromatin conformation during the S phase of the cell cycle. It is possible that the implementation of these techniques will fuel discoveries related to the S phase and DNA replication that were unattainable with the previously available techniques.

An important open question is the causality between topological insulation and transcription, which currently is difficult to properly address. Ideally, a single-locus proteomics approach would be appropriate to investigate the underlying proteome of a TAD border or of a local chromatin insulator region in order to identify candidate insulator factors and analyse whether they have a causal role in determining insulation. Existing single-locus proteomics techniques to study topological insulation and transcription are available, but they are incredibly laborious and complicated to implement^{210–212}. A major breakthrough in proteomics or in wet laboratory protocols to decrease input material is required for single-locus proteomics techniques to become widely applicable. However, this is an exciting lane of research that will certainly help explain the functional aspect of chromatin conformation.

Finally, we argue that not only methods driven by a technological boom but also different and unconventional points of view should coalesce to invent new approaches and fuel milestone discoveries in genome architecture research. The importance of the interdisciplinary approaches described above will become even more prominent with future technological developments. Indeed, in order to reorientate our field of research in the interdisciplinary direction, large consortia are being organized with the purpose of connecting different expertise and points of view. We believe that such developments should be highly encouraged and adopted even in individual laboratories, as they might promote individual projects and, in turn, the field itself.

Published online: 05 May 2021

- Flemming, W. *Zellsubstanz, Kern und Zellteilung* (F. C. W. Vogel, 1882).
- Heitz, E. Das heterochromatin der moose. *Jahrbücher Wissenschaftliche Bot.* **69**, 762–818 (1928).
- Boveri, T. *Die Blastomerenkerne von Ascaris megalocephala und die Theorie der Chromosomenindividualität* (Engelmann, 1909).
- Cremer, T. et al. Analysis of chromosome positions in the interphase nucleus of Chinese hamster cells by laser-UV-microirradiation experiments. *Hum. Genet.* **62**, 201–209 (1982).
- Manuelidis, L. Individual interphase chromosome domains revealed by in situ hybridization. *Hum. Genet.* **71**, 288–293 (1985).
- Schardin, M., Cremer, T., Hager, H. D. & Lang, M. Specific staining of human chromosomes in Chinese hamster × man hybrid cell lines demonstrates interphase chromosome territories. *Hum. Genet.* **71**, 281–287 (1985).
- Cremer, M. et al. Multicolor 3D fluorescence in situ hybridization for imaging interphase chromosomes. *Methods Mol. Biol.* **463**, 205–239 (2012).
- Branco, M. R. & Pombo, A. Intermingling of chromosome territories in interphase suggests role in translocations and transcription-dependent associations. *PLoS Biol.* **4**, e138 (2006).
- Chambeyron, S. & Bickmore, W. A. Chromatin decondensation and nuclear reorganization of the HoxB locus upon induction of transcription. *Genes Dev.* **18**, 1119–1130 (2004).
- Ferrai, C. et al. Poised transcription factories prime silent uPA gene prior to activation. *PLoS Biol.* **8**, e1000270 (2010).
- Rosin, L. F., Nguyen, S. C. & Joyce, E. F. Condensin II drives large-scale folding and spatial partitioning of interphase chromosomes in *Drosophila* nuclei. *PLoS Genet.* **14**, e1007393 (2018).
- Su, J. H., Zheng, P., Kinrot, S. S., Bintu, B. & Zhuang, X. Genome-scale imaging of the 3D organization and transcriptional activity of chromatin. *Cell* **182**, 1641–1659 (2020).
- Fritz, A. J., Sehgal, N., Pliss, A., Xu, J. & Berezney, R. Chromosome territories and the global regulation of the genome. *Genes Chromosom. Cancer* **58**, 407–426 (2019).
- Nguyen, H. Q. et al. 3D mapping and accelerated super-resolution imaging of the human genome using in situ sequencing. *Nat. Methods* **17**, 822–832 (2020).
- This article is the first mention of OligoFISSEQ, showcasing its multiplexing possibilities by imaging 249 loci simultaneously.**
- Takei, Y. et al. Integrated spatial genomics reveals global architecture of single nuclei. *Nature* **590**, 344–350 (2021).
- Payne, A. C. et al. In situ genome sequencing resolves DNA sequence and structure in intact biological samples. *Science* **371**, eaay3446 (2020).
- Cullen, K. E., Klädde, M. P. & Seyfred, M. A. Interaction between transcription regulatory regions of prokaryotic chromatin. *Science* **261**, 203–206 (1993).
- Dekker, J., Rippe, K., Dekker, M. & Kleckner, N. Capturing chromosome conformation. *Science* **295**, 1306–1311 (2002).
- Simonis, M. et al. Nuclear organization of active and inactive chromatin domains uncovered by chromosome conformation capture-on-chip (4C). *Nat. Genet.* **38**, 1348–1354 (2006).
- Dostie, J. et al. Chromosome conformation capture carbon copy (5C): a massively parallel solution for mapping interactions between genomic elements. *Genome Res.* **16**, 1299–1309 (2006).
- Schoenfelder, S. et al. The pluripotent regulatory circuitry connecting promoters to their long-range interacting elements. *Genome Res.* **25**, 582–597 (2015).
- Schoenfelder, S. et al. Polycomb repressive complex PRC1 spatially constrains the mouse embryonic stem cell genome. *Nat. Genet.* **47**, 1179–1186 (2015).
- Mifsud, B. et al. Mapping long-range promoter contacts in human cells with high-resolution capture Hi-C. *Nat. Genet.* **47**, 598–606 (2015).
- Hughes, J. R. et al. Analysis of hundreds of cis-regulatory landscapes at high resolution in a single, high-throughput experiment. *Nat. Genet.* **46**, 205–212 (2014).
- Davies, J. O. J. et al. Multiplexed analysis of chromosome conformation at vastly improved sensitivity. *Nat. Methods* **13**, 74–80 (2015).

26. Jäger, R. et al. Capture Hi-C identifies the chromatin interactome of colorectal cancer risk loci. *Nat. Commun.* **6**, 6178 (2015).
27. Lieberman-Aiden, E. et al. Comprehensive mapping of long-range interactions reveals folding principles of the human genome. *Science* **326**, 289–293 (2009).
28. Duan, Z. et al. A three-dimensional model of the yeast genome. *Nature* **465**, 363–367 (2010).
29. Sati, S. & Cavalli, G. Chromosome conformation capture technologies and their impact in understanding genome function. *Chromosoma* **126**, 33–44 (2017).
30. Horike, S. I., Cai, S., Miyano, M., Cheng, J. F. & Kohwi-Shigematsu, T. Loss of silent-chromatin looping and impaired imprinting of DLX5 in Rett syndrome. *Nat. Genet.* **37**, 31–40 (2005).
31. Fullwood, M. J., Wei, C. L., Liu, E. T. & Ruan, Y. Next-generation DNA sequencing of paired-end tags (PET) for transcriptome and genome analyses. *Genome Res.* **19**, 521–532 (2009).
32. Mumbach, M. R. et al. HiChIP: efficient and sensitive analysis of protein-directed genome architecture. *Nat. Methods* **13**, 919–922 (2016).
33. Fang, R. et al. Mapping of long-range chromatin interactions by proximity ligation-assisted ChIP-seq. *Cell Res* **26**, 1345–1348 (2016).
34. Chen, Y. et al. Mapping 3D genome organization relative to nuclear compartments using TSA-seq as a cytological ruler. *J. Cell Biol.* **217**, 4025–4048 (2018).
This article introduces TSA-seq, a cytological ruler for nuclear speckles and lamina, which is the first genomics method enabling transforming sequencing reads into physical distances in the nucleus.
35. Quinodoz, S. A. et al. Higher-order inter-chromosomal hubs shape 3D genome organization in the nucleus. *Cell* **174**, 744–757 (2018).
36. Arrastia, M. V. et al. A single-cell method to map higher-order 3D genome organization in thousands of individual cells reveals structural heterogeneity in mouse ES cells. Preprint at *bioRxiv* <https://doi.org/10.1101/2020.08.11.242081> (2020).
37. Quinodoz, S. A. et al. RNA promotes the formation of spatial compartments in the nucleus. Preprint at *bioRxiv* <https://doi.org/10.1101/2020.08.25.267435> (2020).
38. Van Steensel, B. & Henikoff, S. Identification of *in vivo* DNA targets of chromatin proteins using tethered Dam methyltransferase. *Nat. Biotechnol.* **14**, 424–428 (2000).
This article introduces DamID, which is used for spatial positioning of heterochromatin protein 1 on chromatin *in vitro* and *in vivo* in *D. melanogaster*.
39. Vogel, M. J., Peric-Hupkes, D. & van Steensel, B. Detection of *in vivo* protein–DNA interactions using DamID in mammalian cells. *Nat. Protoc.* **2**, 1467–1478 (2007).
40. Guelen, L. et al. Domain organization of human chromosomes revealed by mapping of nuclear lamina interactions. *Nature* **453**, 948–951 (2008).
41. Beagrie, R. A. et al. Complex multi-enhancer contacts captured by genome architecture mapping. *Nature* **543**, 519–524 (2017).
This article introduces the GAM method and the discovery of a richness of multiway contacts in the nucleus.
42. Zhang, L. et al. TSA-seq reveals a largely conserved genome organization relative to nuclear speckles with small position changes tightly correlated with gene expression changes. *Genome Res.* **31**, 251–264 (2021).
43. Szabo, Q. et al. TADs are 3D structural units of higher-order chromosome organization in *Drosophila*. *Sci. Adv.* **4**, eaar8082 (2018).
44. Bintu, B. et al. Super-resolution chromatin tracing reveals domains and cooperative interactions in single cells. *Science* **362**, eaau1783 (2018).
This study uses high-throughput oligopaint technology to study chromatin dynamics and shows that TADs are highly stochastic in single cells, but predictable at the population level.
45. Cardozo Gizzi, A. M. et al. Microscopy-based chromosome conformation capture enables simultaneous visualization of genome organization and transcription in intact organisms. *Mol. Cell* **74**, 212–222.e5 (2019).
This article presents highly multiplexed sequential oligopaint FISH (RNA and DNA) based on the conjunction of microscopy and microfluidics in *D. melanogaster* embryos.
46. Nir, G. et al. Walking along chromosomes with super-resolution imaging, contact maps, and integrative modeling. *PLoS Genet.* **14**, e1007872 (2018).
47. Mateo, L. J. et al. Visualizing DNA folding and RNA in embryos at single-cell resolution. *Nature* **568**, 49–54 (2019).
48. Sawh, A. N. et al. Lamina-dependent stretching and unconventional chromosome compartments in early *C. elegans* embryos. *Mol. Cell* **78**, 96–111 (2020).
49. Gu, B. et al. Transcription-coupled changes in nuclear mobility of mammalian *cis*-regulatory elements. *Science* **359**, 1050–1055 (2018).
50. Shaban, H. A. & Seeber, A. Monitoring the spatio-temporal organization and dynamics of the genome. *Nucleic Acids Res.* **48**, 3423–3434 (2020).
51. Barth, R., Bystricky, K. & Shaban, H. A. Coupling chromatin structure and dynamics by live super-resolution imaging. *Sci. Adv.* **6**, eaaz2196 (2020).
52. Vangala, P. et al. High-resolution mapping of multiway enhancer–promoter interactions regulating pathogen detection. *Mol. Cell* **80**, 359–373 (2020).
53. Nora, E. P. et al. Spatial partitioning of the regulatory landscape of the X-inactivation centre. *Nature* **485**, 381–385 (2012).
54. Sexton, T. et al. Three-dimensional folding and functional organization principles of the *Drosophila* genome. *Cell* **148**, 458–472 (2012).
55. Dixon, J. R. et al. Topological domains in mammalian genomes identified by analysis of chromatin interactions. *Nature* **485**, 376–380 (2012).
56. Kalthor, R. et al. Developmental barcoding of whole mouse via homing CRISPR. *Science* **361**, eaat9804 (2018).
57. Szabo, Q. et al. Regulation of single-cell genome organization into TADs and chromatin nanodomains. *Nat. Genet.* **52**, 1151–1157 (2020).
This article is the first description of chromatin nanodomains in mammals using oligopaints in conjunction with SIM.
58. Fudenberg, G. et al. Formation of chromosomal domains by loop extrusion. *Cell Rep.* **15**, 2038–2049 (2016).
59. Wutz, G. et al. Topologically associating domains and chromatin loops depend on cohesin and are regulated by CTCF, WAPL, and PDS5 proteins. *EMBO J.* **36**, 3573–3599 (2017).
60. Rao, S. S. P. et al. Cohesin loss eliminates all loop domains. *Cell* **171**, 305–320 (2017).
61. Schwarzer, W. et al. Two independent modes of chromatin organization revealed by cohesin removal. *Nature* **551**, 51–56 (2017).
62. Guo, Y. et al. CRISPR inversion of CTCF sites alters genome topology and enhancer/promoter function. *Cell* **162**, 900–910 (2015).
63. Haahrhuis, J. H. I. et al. The cohesin release factor WAPL restricts chromatin loop extension. *Cell* **169**, 693–707 (2017).
64. Nora, E. P. et al. Targeted degradation of CTCF decouples local insulation of chromosome domains from genomic compartmentalization. *Cell* **169**, 930–944 (2017).
65. Bonev, B. et al. Multiscale 3D genome rewiring during mouse article multiscale 3D genome rewiring during mouse neural development. *Cell* **171**, 557–572 (2017).
66. Ulianov, S. V. et al. Active chromatin and transcription play a key role in chromosome partitioning into topologically associating domains. *Genome Res.* **26**, 70–84 (2016).
67. Sanborn, A. L. et al. Chromatin extrusion explains key features of loop and domain formation in wild-type and engineered genomes. *Proc. Natl Acad. Sci. USA* **112**, 6456–6465 (2015).
68. Nuebler, J., Fudenberg, G., Imakaev, M., Abdennur, N. & Mirny, L. A. Chromatin organization by an interplay of loop extrusion and compartmental segregation. *Proc. Natl Acad. Sci. USA* **115**, 6697–6706 (2018).
69. Rowley, M. J. et al. Evolutionarily conserved principles predict 3D chromatin organization. *Mol. Cell* **67**, 837–852 (2017).
70. Benedetti, F., Racko, D., Dorier, J., Burnier, Y. & Stasiak, A. Transcription-induced supercoiling explains formation of self-interacting chromatin domains in *S. pombe*. *Nucleic Acids Res.* **45**, 9850–9859 (2017).
71. Szabo, Q., Bantignies, F. & Cavalli, G. Principles of genome folding into topologically associating domains. *Sci. Adv.* **5**, eaaw1668 (2019).
72. Jerković, I., Szabo, Q., Bantignies, F. & Cavalli, G. Higher-order chromosomal structures mediate genome function. *J. Mol. Biol.* **432**, 676–681 (2020).
73. Oomen, M. E., Hedger, A. K., Watts, J. K. & Dekker, J. Detecting chromatin interactions between and along sister chromatids with SisterC. *Nat. Methods* **17**, 1002–1009 (2020).
74. Mitter, M. et al. Conformation of sister chromatids in the replicated human genome. *Nature* **586**, 139–144 (2020).
75. AlHaj Abed, J. et al. Highly structured homolog pairing reflects functional organization of the *Drosophila* genome. *Nat. Commun.* **10**, 1–14 (2019).
76. Franke, M. et al. Formation of new chromatin domains determines pathogenicity of genomic duplications. *Nature* **538**, 265–269 (2016).
77. Lupiáñez, D. G., Spielmann, M. & Mundlos, S. Breaking TADs: how alterations of chromatin domains result in disease. *Trends Genet.* **32**, 225–237 (2016).
78. Despang, A. et al. Functional dissection of the Sox9–Kcnj2 locus identifies nonessential and instructive roles of TAD architecture. *Nat. Genet.* **51**, 1263–1271 (2019).
79. Andrey, G. & Mundlos, S. The three-dimensional genome: regulating gene expression during pluripotency and development. *Development* **144**, 3646–3658 (2017).
80. Weischenfeldt, J. et al. Pan-cancer analysis of somatic copy-number alterations implicates IRS4 and IGF2 in enhancer hijacking. *Nat. Genet.* **49**, 65–74 (2016).
81. Liu, X. S. et al. Rescue of fragile X syndrome neurons by DNA methylation editing of the FMR1 gene. *Cell* **172**, 979–992 (2018).
82. Bruneau, B. G. & Nora, E. P. Chromatin domains go on repeat in disease. *Cell* **175**, 38–40 (2018).
83. Akdemir, K. C. et al. Somatic mutation distributions in cancer genomes vary with three-dimensional chromatin structure. *Nat. Genet.* **52**, 1178–1188 (2020).
84. Valton, A. L. & Dekker, J. TAD disruption as oncogenic driver. *Curr. Opin. Genet. Dev.* **36**, 34–40 (2016).
85. Rao, S. S. P. et al. A 3D map of the human genome at kilobase resolution reveals principles of chromatin looping. *Cell* **159**, 1665–1680 (2014).
This paper showcases the first use of the *in situ* Hi-C protocol and introduces HiCCUPS, a contact caller dedicated to chromatin loops.
86. Nagano, T. et al. Comparison of Hi-C results using *in-solution* versus *in-nucleus* ligation. *Genome Biol.* **16**, 175 (2015).
87. Nagano, T. et al. Single-cell Hi-C reveals cell-to-cell variability in chromosome structure. *Nature* **502**, 59–64 (2015).
88. Ma, W. et al. Fine-scale chromatin interaction maps reveal the *cis*-regulatory landscape of human lincRNA genes. *Nat. Methods* **12**, 71–78 (2014).
89. Ramani, V. et al. Mapping 3D genome architecture through *in situ* DNase Hi-C. *Nat. Protoc.* **11**, 2104–2121 (2016).
90. Deng, X. et al. Bipartite structure of the inactive mouse X chromosome. *Genome Biol.* **16**, 152 (2015).
91. Hsieh, T. H. S. et al. Mapping nucleosome resolution chromosome folding in yeast by Micro-C. *Cell* **162**, 108–119 (2015).
92. Hsieh, T. H. S. et al. Resolving the 3D landscape of transcription-linked mammalian chromatin folding. *Mol. Cell* **78**, 539–553 (2020).
This article presents high-resolution Micro-C performed in mouse embryonic stem cells with concomitant analysis of nucleosome positioning.
93. Krietenstein, N. et al. Ultrastructural details of mammalian chromosome architecture. *Mol. Cell* **78**, 554–565 (2020).
This article presents high-resolution Micro-C performed in human embryonic stem cells and fibroblasts with concomitant analysis of nucleosome positioning.
94. Goel, V. Y. & Hansen, A. S. The macro and micro of chromosome conformation capture. *WIREs Dev. Biol.* <https://doi.org/10.1002/wdev.395> (2020).
95. Akgol Oksuz, B. et al. Systematic evaluation of chromosome conformation capture assays. Preprint at *bioRxiv* <https://doi.org/10.1101/2020.12.26.424448> (2020).
96. Baranello, L., Kouzine, F., Sanford, S. & Levens, D. ChIP bias as a function of cross-linking time. *Chromosom. Res.* **24**, 175–181 (2016).
97. Gavrilov, A., Razin, S. V. & Cavalli, G. *In vivo* formaldehyde cross-linking: it is time for black box analysis. *Brief. Funct. Genomics* **14**, 163–165 (2015).

98. Kempfer, R. & Pombo, A. Methods for mapping 3D chromosome architecture. *Nat. Rev. Genet.* **21**, 207–226 (2020).
99. Fullwood, M. J. & Ruan, Y. ChIP-based methods for the identification of long-range chromatin interactions. *J. Cell. Biochem.* **107**, 30–39 (2009).
100. Kind, J. et al. Genome-wide maps of nuclear lamina interactions in single human cells. *Cell* **163**, 134–147 (2015).
101. Redolfi, J. et al. DamC reveals principles of chromatin folding in vivo without crosslinking and ligation. *Nat. Struct. Mol. Biol.* **26**, 471–480 (2019).
102. Li, X. et al. Long-read ChIA-PET for base-pair-resolution mapping of haplotype-specific chromatin interactions. *Nat. Protoc.* **12**, 899–915 (2017).
103. Andrey, G. et al. Characterization of hundreds of regulatory landscapes in developing limbs reveals two regimes of chromatin folding. *Genome Res.* **27**, 223–235 (2017).
104. Rooijers, K. et al. Simultaneous quantification of protein–DNA contacts and transcriptomes in single cells. *Nat. Biotechnol.* **37**, 766–772 (2019).
105. Sahl, S. J., Hell, S. W. & Jakobs, S. Fluorescence nanoscopy in cell biology. *Nat. Rev. Mol. Cell Biol.* **18**, 685–701 (2017).
106. Liu, Z., Lavis, L. D. & Betzig, E. Imaging live-cell dynamics and structure at the single-molecule level. *Mol. Cell* **58**, 644–659 (2015).
107. Heintzmann, R. & Cremer, C. G. Laterally modulated excitation microscopy: improvement of resolution by using a diffraction grating. *Proc. SPIE* **3568**, 185–196 (1999).
108. Gustafsson, M. G. L. Surpassing the lateral resolution limit by a factor of two using structured illumination microscopy. *J. Microsc.* **198**, 82–87 (2000).
109. Gustafsson, M. G. L. et al. Three-dimensional resolution doubling in wide-field fluorescence microscopy by structured illumination. *Biophys. J.* **94**, 4957–4970 (2008).
110. Schermelleh, L. et al. Subdiffraction multicolor imaging of the nuclear periphery with 3D structured illumination microscopy. *Science* **320**, 1332–1336 (2008).
111. Miron, E. et al. Chromatin arranges in chains of mesoscale domains with nanoscale functional topography independent of cohesin. *Sci. Adv.* **6**, eaba8811 (2020).
112. Rust, M. J., Bates, M. & Zhuang, X. Sub-diffraction-limit imaging by stochastic optical reconstruction microscopy (STORM). *Nat. Methods* **3**, 793–795 (2006).
113. Betzig, E. et al. Imaging intracellular fluorescent proteins at nanometer resolution. *Science* **313**, 1642–1645 (2006).
114. Hess, S. T., Girirajan, T. P. K. & Mason, M. D. Ultra-high resolution imaging by fluorescence photoactivation localization microscopy. *Biophys. J.* **91**, 4258–4272 (2006).
115. Huang, B., Babcock, H. & Zhuang, X. Breaking the diffraction barrier: super-resolution imaging of cells. *Cell* **143**, 1047–1058 (2010).
116. Ricci, M. A., Manzo, C., Lakadamyali, M. & Cosma, M. P. Chromatin fibers are formed by heterogeneous groups of nucleosomes in vivo. *Cell* **160**, 1145–1158 (2015).
117. Nozaki, T. et al. Dynamic organization of chromatin domains revealed by super-resolution live-cell imaging. *Mol. Cell* **67**, 282–293 (2017).
118. Hell, S. W. & Wichmann, J. Breaking the diffraction resolution limit by stimulated emission: stimulated-emission-depletion fluorescence microscopy. *Opt. Lett.* **19**, 780–782 (1994).
119. Klar, T. A., Jakobs, S., Dyba, M., Egner, A. & Hell, S. W. Fluorescence microscopy with diffraction resolution barrier broken by stimulated emission. *Proc. Natl Acad. Sci. USA* **97**, 8206–8210 (2000).
120. Hofmann, M., Eggeling, C., Jakobs, S. & Hell, S. W. Breaking the diffraction barrier in fluorescence microscopy at low light intensities by using reversibly photoswitchable proteins. *Proc. Natl Acad. Sci. USA* **102**, 17565–17569 (2005).
121. Gwosch, C. K. et al. MINFLUX nanoscopy delivers multicolor nanometer 3D-resolution in (living) cells. *Nat. Methods* **17**, 217–224 (2020).
122. Beliveau, B. J. et al. Versatile design and synthesis platform for visualizing genomes with Oligopaint FISH probes. *Proc. Natl Acad. Sci. USA* **109**, 21301–21306 (2012).
123. Wang, S. et al. Spatial organization of chromatin domains and compartments in single chromosomes. *Science* **353**, 598–602 (2016).
124. Ou, H. D. et al. ChromEMF: visualizing 3D chromatin structure and compaction in interphase and mitotic cells. *Science* **357**, eaag0025 (2017).
125. Yaffe, E. & Tanay, A. Probabilistic modeling of Hi-C contact maps eliminates systematic biases to characterize global chromosomal architecture. *Nat. Genet.* **43**, 1059–1065 (2011).
126. Imakaev, M. et al. Iterative correction of Hi-C data reveals hallmarks of chromosome organization. *Nat. Methods* **9**, 999–1003 (2012).
127. Ryba, T. et al. Evolutionarily conserved replication timing profiles predict long-range chromatin interactions and distinguish closely related cell types. *Genome Res.* **20**, 761–770 (2010).
128. Di Pierro, M., Cheng, R. R., Aiden, E. L., Wolyne, P. G. & Onuchic, J. N. De novo prediction of human chromosome structures: epigenetic marking patterns encode genome architecture. *Proc. Natl Acad. Sci. USA* **114**, 12126–12131 (2017).
129. Lin, D., Bonora, G., Yardimci, G. G. & Noble, W. S. Computational methods for analyzing and modeling genome structure and organization. *Wiley Interdiscip. Rev. Syst. Biol. Med.* **11**, e1435 (2019).
130. Kalhor, R., Tjong, H., Jayathilaka, N., Alber, F. & Chen, L. Genome architectures revealed by tethered chromosome conformation capture and population-based modeling. *Nat. Biotechnol.* **30**, 90–98 (2012).
131. Crane, E. et al. Condensin-driven remodelling of X chromosome topology during dosage compensation. *Nature* **523**, 240–244 (2015).
132. Shin, H. et al. TopDom: an efficient and deterministic method for identifying topological domains in genomes. *Nucleic Acids Res.* **44**, e70 (2015). **This article presents one of the most reliable and popular TAD callers.**
133. Malik, L. & Patro, R. Rich chromatin structure prediction from Hi-C data. *IEEE/ACM Trans. Comput. Biol. Bioinform.* **16**, 1448–1458 (2019).
134. Haddad, N., Vaillant, C. & Jost, D. IC-Finder: inferring robustly the hierarchical organization of chromatin folding. *Nucleic Acids Res.* **45**, 81 (2017).
135. Soler-Vila, P., Cuscó, P., Farabella, I., Di Stefano, M. & Marti-Renom, M. A. Hierarchical chromatin organization detected by TADpole. *Nucleic Acids Res.* **48**, e39 (2020). **This paper presents one of the most recently developed TAD callers and is extremely valuable for its benchmarking quality and for multiple TAD caller comparisons.**
136. Norton, H. K. et al. Detecting hierarchical genome folding with network modularity. *Nat. Methods* **15**, 119–122 (2018).
137. Moller, J. & de Pablo, J. J. Bottom-up meets top-down: the crossroads of multiscale chromatin modeling. *Biophys. J.* **118**, 2057–2065 (2020).
138. Bendandi, A., Dante, S., Zia, S. R., Diaspro, A. & Rocchia, W. Chromatin compaction multiscale modeling: a complex synergy between theory, simulation, and experiment. *Front. Mol. Biosci.* **7**, 15 (2020).
139. Zufferey, M., Tavernari, D., Orichio, E. & Ciriello, G. Comparison of computational methods for the identification of topologically associating domains. *Genome Biol.* **19**, 217 (2018).
140. Forcato, M. et al. Comparison of computational methods for Hi-C data analysis. *Nat. Methods* **14**, 679–685 (2017).
141. Ay, F., Bailey, T. L. & Noble, W. S. Statistical confidence estimation for Hi-C data reveals regulatory chromatin contacts. *Genome Res.* **24**, 999–1011 (2014).
142. Carty, M. et al. An integrated model for detecting significant chromatin interactions from high-resolution Hi-C data. *Nat. Commun.* **8**, 1–10 (2017).
143. Pal, K., Forcato, M. & Ferrari, F. Hi-C analysis: from data generation to integration. *Biophys. Rev.* **11**, 67–78 (2019).
144. Dozmorov, M., Sirusb & Benfeitas, R. Hi-C data analysis tools and papers. *GitHub* https://github.com/mdozmorov/HiC_tools/blob/master/README.md (2021).
145. Roayaei Ardakany, A., Gezer, H. T., Lonardi, S. & Ay, F. Mustache: multi-scale detection of chromatin loops from Hi-C and Micro-C maps using scale-space representation. *Genome Biol.* **21**, 256 (2020).
146. Jordan Rowley, M. et al. Analysis of Hi-C data using SIP effectively identifies loops in organisms from *C. elegans* to mammals. *Genome Res.* **30**, 447–458 (2020).
147. Ay, F. & Noble, W. S. Analysis methods for studying the 3D architecture of the genome. *Genome Biol.* **16**, 183 (2015).
148. Nikumbh, S. & Pfeifer, N. Genetic sequence-based prediction of long-range chromatin interactions suggests a potential role of short tandem repeat sequences in genome organization. *BMC Bioinformatics* **18**, 218 (2017).
149. Rhie, S. K. et al. Using 3D epigenomic maps of primary olfactory neuronal cells from living individuals to understand gene regulation. *Sci. Adv.* **4**, eaav8550 (2018).
150. Hafez, D. et al. McEnhancer: predicting gene expression via semi-supervised assignment of enhancers to target genes. *Genome Biol.* **18**, 199 (2017).
151. Di Iulio, J. et al. The human noncoding genome defined by genetic diversity. *Nat. Genet.* **50**, 333–337 (2018).
152. Javierre, B. M. et al. Lineage-specific genome architecture links enhancers and non-coding disease variants to target gene promoters. *Cell* **167**, 1369–1384 (2016).
153. Mitchelmore, J., Grinberg, N. F., Wallace, C. & Spivakov, M. Functional effects of variation in transcription factor binding highlight long-range gene regulation by e-promoters. *Nucleic Acids Res.* **48**, 2866–2879 (2020).
154. Malysheva, V., Mendoza-Parra, M. A., Blum, M., Spivakov, M. & Gronemeyer, H. Gene regulatory network reconstruction incorporating 3D chromosomal architecture reveals key transcription factors and DNA elements driving neural lineage commitment. Preprint at *bioRxiv* <https://doi.org/10.1101/303842> (2019).
155. Madrid-Mencia, M., Raineri, E., Cao, T. B. N. & Pancaldi, V. Using GARDEN-NET and ChAseR to explore human haematopoietic 3D chromatin interaction networks. *Nucleic Acids Res.* **48**, 4066–4080 (2020).
156. Zhang, Y. et al. Enhancing Hi-C data resolution with deep convolutional neural network HiCPlus. *Nat. Commun.* **9**, 1–9 (2018).
157. Oluwadare, O., Highsmith, M. & Cheng, J. An overview of methods for reconstructing 3-D chromosome and genome structures from Hi-C data. *Biol. Proced. Online* **21**, 1–20 (2019).
158. Marti-Renom, M. A. et al. Challenges and guidelines toward 4D nucleome data and model standards. *Nat. Genet.* **50**, 1352–1358 (2018).
159. MacPherson, O., Beltran, B. & Spakowitz, A. J. Bottom-up modeling of chromatin segregation due to epigenetic modifications. *Proc. Natl Acad. Sci. USA* **115**, 12739–12744 (2018).
160. Bianco, S., Chiariello, A. M., Annunziatella, C., Esposito, A. & Nicodemi, M. Predicting chromatin architecture from models of polymer physics. *Chromosome Res.* **25**, 25–34 (2017).
161. Mirny, L. A. The fractal globule as a model of chromatin architecture in the cell. *Chromosom. Res.* **19**, 37–51 (2011).
162. Barbieri, M. et al. A model of the large-scale organization of chromatin. *Biochem. Soc. Trans.* **41**, 508–512 (2013).
163. Jost, D., Carrivain, P., Cavalli, G. & Vaillant, C. Modeling epigenome folding: formation and dynamics of topologically associated chromatin domains. *Nucleic Acids Res.* **42**, 9553–9561 (2014).
164. Jost, D. & Vaillant, C. Epigenomics in 3D: importance of long-range spreading and specific interactions in epigenomic maintenance. *Nucleic Acids Res.* **46**, 2252–2264 (2018).
165. Barbieri, M. et al. Active and poised promoter states drive folding of the extended HoxB locus in mouse embryonic stem cells. *Nat. Struct. Mol. Biol.* **24**, 515–524 (2017).
166. Falk, M. et al. Heterochromatin drives compartmentalization of inverted and conventional nuclei. *Nature* **570**, 395–399 (2019).
167. Oliveira Junior, A. B., Contessoto, V. G., Mello, M. F. & Onuchic, J. N. A scalable computational approach for simulating complexes of multiple chromosomes. *J. Mol. Biol.* **433**, 166700 (2020).
168. Ghosh, S. K. & Jost, D. How epigenome drives chromatin folding and dynamics, insights from efficient coarse-grained models of chromosomes. *PLoS Comput. Biol.* **14**, e1006159 (2018).
169. Giorgetti, L. et al. Predictive polymer modeling reveals coupled fluctuations in chromosome conformation and transcription. *Cell* **157**, 950–963 (2014).
170. Bianco, S. et al. Polymer physics predicts the effects of structural variants on chromatin architecture. *Nat. Genet.* **50**, 662–667 (2018).
171. Contessoto, V. G. et al. The Nucleome Data Bank: web-based resources to simulate and analyze the three-dimensional genome. *Nucleic Acids Res.* **49**, 172–182 (2020).

172. Rousseau, M., Fraser, J., Ferraiuolo, M. A., Dostie, J. & Blanchette, M. Three-dimensional modeling of chromatin structure from interaction frequency data using Markov chain Monte Carlo sampling. *BMC Bioinformatics* **12**, 414 (2011).
173. Baú, D. et al. The three-dimensional folding of the α -globin gene domain reveals formation of chromatin globules. *Nat. Struct. Mol. Biol.* **18**, 107–115 (2011).
174. Trussart, M. et al. Defined chromosome structure in the genome-reduced bacterium *Mycoplasma pneumoniae*. *Nat. Commun.* **8**, 14665 (2017).
175. Zhu, G. et al. Reconstructing spatial organizations of chromosomes through manifold learning. *Nucleic Acids Res.* **46**, e50 (2018).
176. Paulsen, J. et al. Long-range interactions between topologically associating domains shape the four-dimensional genome during differentiation. *Nat. Genet.* **51**, 835–843 (2019).
177. Lesne, A., Riposo, J., Roger, P., Cournac, A. & Mozziconacci, J. 3D genome reconstruction from chromosomal contacts. *Nat. Methods* **11**, 1141–1143 (2014).
178. Trieu, T., Oluwadare, O. & Cheng, J. Hierarchical reconstruction of high-resolution 3D models of large chromosomes. *Sci. Rep.* **9**, 1–12 (2019).
179. Tan, L., Xing, D., Chang, C.-H. H., Li, H. & Xie, X. S. Three-dimensional genome structures of single diploid human cells. *Science* **361**, 924–928 (2018).
180. Di Stefano, M. et al. Transcriptional activation during cell reprogramming correlates with the formation of 3D open chromatin hubs. *Nat. Commun.* **11**, 1–12 (2020).
181. Li, Q. et al. The three-dimensional genome organization of *Drosophila melanogaster* through data integration. *Genome Biol.* **18**, 145 (2017).
182. Hua, N. et al. Producing genome structure populations with the dynamic and automated PGS software. *Nat. Protoc.* **13**, 915–926 (2018).
183. Whalen, S., Truty, R. M. & Pollard, K. S. Enhancer–promoter interactions are encoded by complex genomic signatures on looping chromatin. *Nat. Genet.* **48**, 488–496 (2016).
184. Li, W., Wong, W. H. & Jiang, R. DeepTACT: predicting 3D chromatin contacts via bootstrapping deep learning. *Nucleic Acids Res.* **47**, e60 (2019).
185. Fudenberg, G., Kelley, D. R. & Pollard, K. S. Predicting 3D genome folding from DNA sequence with Akita. *Nat. Methods* **17**, 1111–1117 (2020). **This is the first computational modelling paper describing modelling of chromatin conformation solely from the DNA.**
186. Schwessinger, R. et al. DeepC: predicting 3D genome folding using megabase-scale transfer learning. *Nat. Methods* **17**, 1118–1124 (2020). **This article presents one of the first computational tools to model chromatin conformation solely from the DNA sequence. However, unlike Akita, it requires training on the epigenetics data.**
187. Zhang, S., Chasman, D., Knaack, S. & Roy, S. In silico prediction of high-resolution Hi-C interaction matrices. *Nat. Commun.* **10**, 1–18 (2019).
188. Belokopytova, P. S., Nuriddinov, M. A., Mozheiko, E. A., Fishman, D. & Fishman, V. Quantitative prediction of enhancer–promoter interactions. *Genome Res.* **30**, 72–84 (2020).
189. Qi, Y. et al. Data-driven polymer model for mechanistic exploration of diploid genome organization. *Biophys. J.* **119**, 1905–1916 (2020).
190. de Luca, K. L. & Kind, J. in *Methods in Molecular Biology* Vol. 2157 159–172 (Humana, 2021).
191. Li, G. et al. Joint profiling of DNA methylation and chromatin architecture in single cells. *Nat. Methods* **16**, 991–993 (2019).
192. Zheng, M. et al. Multiplex chromatin interactions with single-molecule precision. *Nature* **566**, 558–562 (2019).
193. Ramani, V. et al. Massively multiplex single-cell Hi-C. *Nat. Methods* **14**, 263–266 (2017).
194. You, Q. et al. Direct DNA crosslinking with CAP-C uncovers transcription-dependent chromatin organization at high resolution. *Nat. Biotechnol.* **39**, 225–235 (2020).
195. Girelli, G. et al. GPSeq reveals the radial organization of chromatin in the cell nucleus. *Nat. Biotechnol.* **38**, 1184–1193 (2020).
196. Wang, Y. et al. SPIN reveals genome-wide landscape of nuclear compartmentalization. *Genome Biol.* **22**, 36 (2021). **This article presents the first tool that combines nuclear architecture (positioning) data from**
- TSA-seq and DamID in order to compute spatial compartmentalization of chromatin in respect to the lamina or nuclear bodies such as nuclear speckles.**
197. Kubalová, I. et al. Prospects and limitations of expansion microscopy in chromatin ultrastructure determination. *Chromosom. Res.* **28**, 355–368 (2020).
198. Shi, X. et al. Label-retention expansion microscopy. Preprint at *bioRxiv* <https://doi.org/10.1101/687954> (2021).
199. Wassie, A. T., Zhao, Y. & Boyden, E. S. Expansion microscopy: principles and uses in biological research. *Nat. Methods* **16**, 33–41 (2019).
200. Alon, S. et al. Expansion sequencing: spatially precise in situ transcriptomics in intact biological systems. *Science* **371**, eaax2656 (2021).
201. Robinett, C. C. et al. In vivo localization of DNA sequences and visualization of large-scale chromatin organization using lac operator/repressor recognition. *J. Cell Biol.* **135**, 1685–1700 (1996).
202. Belmont, A. S. & Straight, A. F. In vivo visualization of chromosomes using lac operator-repressor binding. *Trends Cell Biol.* **8**, 121–124 (1998).
203. Lucas, J. S., Zhang, Y., Dudko, O. K. & Murre, C. 3D trajectories adopted by coding and regulatory DNA elements: first-passage times for genomic interactions. *Cell* **158**, 339–352 (2014).
204. Chen, H. et al. Dynamic interplay between enhancer–promoter topology and gene activity. *Nat. Genet.* **50**, 1296–1303 (2018).
205. Maass, P. G. et al. Spatiotemporal allele organization by allele-specific CRISPR live-cell imaging (SNP-CLING). *Nat. Struct. Mol. Biol.* **25**, 176–184 (2018).
206. Wang, H. et al. CRISPR-mediated live imaging of genome editing and transcription. *Science* **365**, 1301–1305 (2019).
207. Geng, Y. & Pertsinidis, A. CAS-LiveFISH: simple and versatile imaging of genomic loci in live mammalian cells and early pre-implantation embryos. Preprint at *bioRxiv* <https://doi.org/10.1101/2020.08.25.265306> (2020).
208. Neguembor, M. V. et al. (Po)STAC (polycistronic SunTag modified CRISPR) enables live-cell and fixed-cell super-resolution imaging of multiple genes. *Nucleic Acids Res.* **46**, e30 (2018).
209. Chu, L. et al. The 3D topography of mitotic chromosomes. *Mol. Cell* **79**, 902–916.e6 (2020).
210. Liu, X. et al. In situ capture of chromatin interactions by biotinylated dCas9. *Cell* **170**, 1028–1043 (2017).
211. Tsui, C. et al. dCas9-targeted locus-specific protein isolation method identifies histone gene regulators. *Proc. Natl Acad. Sci. USA* **115**, 2734–2741 (2018).
212. Myers, S. A. et al. Discovery of proteins associated with a predefined genomic locus via dCas9–APEX-mediated proximity labeling. *Nat. Methods* **15**, 437–439 (2018).
213. de Wit, E. et al. CTCF binding polarity determines chromatin looping. *Mol. Cell* **60**, 676–684 (2015).
214. Gómez-Marín, C. et al. Evolutionary comparison reveals that diverging CTCF sites are signatures of ancestral topological associating domains borders. *Proc. Natl Acad. Sci. USA* **112**, 7542–7547 (2015).
215. Bantignies, F. et al. Polycomb-dependent regulatory contacts between distant hox loci in *Drosophila*. *Cell* **144**, 214–226 (2011).
216. Monahan, K., Horta, A. & Lovmardas, S. LHX2- and LDB1-mediated *trans* interactions regulate olfactory receptor choice. *Nature* **565**, 448–453 (2019).
217. Phillips-Cremins, J. E. et al. Architectural protein subclasses shape 3D organization of genomes during lineage commitment. *Cell* **153**, 1281–1295 (2013).
218. Bhattacharyya, S., Chandra, V., Vijayanand, P. & Ay, F. Identification of significant chromatin contacts from HiChIP data by FiHiChIP. *Nat. Commun.* **10**, 1–14 (2019).
219. Takei, Y. et al. Global architecture of the nucleus in single cells by DNA seqFISH+ and multiplexed immunofluorescence. Preprint at *bioRxiv* <https://doi.org/10.1101/2020.11.29.403055> (2020).
220. Tolhuis, B., Palstra, R. J., Splinter, E., Grosveld, F. & de Laat, W. Looping and interaction between hypersensitive sites in the active β -globin locus. *Mol. Cell* **10**, 1453–1465 (2002).
221. Palstra, R. J. et al. The β -globin nuclear compartment in development and erythroid differentiation. *Nat. Genet.* **35**, 190–194 (2003).
222. Splinter, E. et al. CTCF mediates long-range chromatin looping and local histone modification in the β -globin locus. *Genes Dev.* **20**, 2349–2354 (2006).
223. Vakoc, C. R. et al. Proximity among distant regulatory elements at the β -globin locus requires GATA-1 and FOG-1. *Mol. Cell* **17**, 453–462 (2005).
224. Splinter, E. & De Laat, W. The complex transcription regulatory landscape of our genome: control in three dimensions. *EMBO J.* **30**, 4345–4355 (2011).
225. Zhao, Z. et al. Circular chromosome conformation capture (4C) uncovers extensive networks of epigenetically regulated intra- and interchromosomal interactions. *Nat. Genet.* **38**, 1341–1347 (2006).
226. Andrey, G. et al. A switch between topological domains underlies HoxD genes collinearity in mouse limbs. *Science* **340**, 1234167 (2013).
227. Ghavi-Helm, Y. et al. Enhancer loops appear stable during development and are associated with paused polymerase. *Nature* **512**, 96–100 (2014).
228. Apostolou, E. et al. Genome-wide chromatin interactions of the nanog locus in pluripotency, differentiation, and reprogramming. *Cell Stem Cell* **12**, 699–712 (2013).
229. Van De Werken, H. J. G. et al. in *Methods in Enzymology* Vol. 513 (eds Wu, C. & Allis, D.) 89–112 (Academic, 2012).
230. Bonev, B. & Cavalli, G. Organization and function of the 3D genome. *Nat. Rev. Genet.* **17**, 661–678 (2016).
231. Y. G. H. et al. Highly rearranged chromosomes reveal uncoupling between genome topology and gene expression. *Nat. Genet.* **51**, 1272–1282 (2019).
232. Lupiáñez, D. G. et al. Disruptions of topological chromatin domains cause pathogenic rewiring of gene–enhancer interactions. *Cell* **161**, 1012–1025 (2015).
233. Ogiyama, Y., Schuettengruber, B., Papadopoulos, G. L., Chang, J.-M. & Cavalli, G. Polycomb-dependent chromatin looping contributes to gene silencing during *Drosophila* development. *Mol. Cell* **71**, 73–88 (2018).
234. Flavahan, W. A. et al. Altered chromosomal topology drives oncogenic programs in SDH-deficient GISTs. *Nature* **575**, 229–233 (2019).
235. Tarjan, D. R., Flavahan, W. A. & Bernstein, B. E. Epigenome editing strategies for the functional annotation of CTCF insulators. *Nat. Commun.* **10**, 4258 (2019).
236. Kim, J. H. et al. LADL: light-activated dynamic looping for endogenous gene expression control. *Nat. Methods* **16**, 633–639 (2019).
237. Wang, H. et al. CRISPR-mediated programmable 3D genome positioning and nuclear organization. *Cell* **175**, 1405–1417 (2018).

Acknowledgements

The authors thank M. Di Stefano for critical reading of the Computational analysis and modelling section, B. Schuettengruber and F. Bantignies for input on figures, and O. Szabo for help with and input on Fig. 4. I.J. was supported by an European Molecular Biology Organization (EMBO) Long-Term Fellowship (ALTF 559-2018) and the Laboratory of Excellence EpiGenMed. Research in the G.C. laboratory is supported by grants from the European Research Council (Advanced Grant 3DEpi, under grant agreement No 788972), the European Union's Horizon 2020 research and innovation programme (MuG, under grant agreement No 676556 and ChromDesign, under the Marie Skłodowska-Curie grant agreement No 813327), the Agence Nationale de la Recherche (ANR-15-CE12-0006 EpiDevoMath), the Fondation pour la Recherche Médicale (DEI20151234396), the MSDAVENIR foundation (Project GENE-IGH), the INSERM and the French National Cancer Institute (INCA).

Author contributions

The authors contributed equally to all aspects of the article.

Competing interests

The authors declare no competing interests.

Peer review information

Nature Reviews Molecular Cell Biology thanks Zhijun Duan, Bing Ren, Juan Vaquerizas, who co-reviewed with Elizabeth Ing-Simmons, and the other, anonymous reviewer(s) for their contribution to the peer review of this work.

Publisher's note

Springer Nature remains neutral with regard to jurisdictional claims in published maps and institutional affiliations.

© Springer Nature Limited 2021